DOI: 10.1002/ejic.200900395

Copper Complexes with Neutral N4 Tripodal Ligands: Influence of the Number of Nitrogen Donors on Their Structures, Properties, and Reactivity

Kiyoshi Fujisawa,*[a] Shingo Chiba,[a] Yoshitaro Miyashita,[a] and Ken-ichi Okamoto[a]

Dedicated to Professor Kenneth D. Karlin on the occasion of his 60th birthday

Keywords: Copper / N ligands / Ligand effects / Coordination modes / Structure elucidation / Electronic structure

Copper coordination complexes of the neutral tetradentate nitrogen-containing ligands tris(3,5-dimethylpyrazol-1-ylmethyl)amine (L0N4) and tris(3,5-diisopropylpyrazol-1-ylmethyl)amine (L1N4), namely the copper(II) chlorido complexes $[Cu^{II}(L0N4)Cl_2]$ (**1**) and $[Cu^{II}(L1N4)Cl_2]$ (**2**), the copper(II) nitrato complexes $[Cu^{II}(L0N4)(NO_3)](NO_3)$ (**3**) and $[Cu^{II}(L1N4)(NO_3)](NO_3)$ (**4**), and the copper(II) sulfato complexes $[Cu^{II}(L0N4)(SO_4)]$ (**5**) and $[Cu^{II}(L1N4)(SO_4)]$ (**6**), and the copper(I) complexes $[Cu^{I}(L0N4)](PF_6)$ (**7**) and $[Cu^{I}(L0N4)(PPh_3)](ClO_4)$ (**8**), have been systematically synthesized in order to investigate the influence of the number of nitrogen donors on their structures, properties, and reactivity. All copper(II) complexes were fully characterized by X-ray crystallography and by IR/far-IR, UV/Vis absorption, and ESR spectroscopy. Although the structure of **7** was not determined by X-ray crystallography, this complex and the structurally characterized copper(I) triphenylphosphane complex **8** were fully characterized by IR/far-IR and NMR spectroscopy. A comparison of the copper(II) complexes with two tris(pyrazol-1-ylmethyl)amine ligands with different bulkiness of the pyrazolyl rings has allowed us to evaluate the second coordination sphere effects of the ligands. Moreover, the structures and physicochemical properties of these complexes are compared with those of related complexes containing the neutral tridentate tris(pyrazolyl)methane ligand and the neutral bidentate bis(pyrazolyl)methane ligand. Finally, the relative stability of the copper(I) complexes is discussed. The influence of the number of nitrogen donors in copper complexes is observed from these systematic results.

Introduction

Copper is one of the most important elements in the field of biological systems and also for laboratory and industrial use. Indeed, the structures and functions of many copper-containing proteins have been resolved during the past decades.[1–5] These structures contain many different ligand donor sets coordinated to the copper centers with a variety of coordination numbers and elements as well as coordination modes. It is therefore of great interest to determine how structure and function are influenced by the number of coordinating atoms around the copper centers.

Hydrotris(pyrazolyl)borate (tpzb) ligands, which readily coordinate to metal ions as a face-capping tridentate ligand, are one of the most widely used ligands for coordination compounds.[6–11] The tpzb anion is a six-electron donor ligand whose pyrazolyl rings can be substituted with bulky groups, especially at the 3- and/or 5-position(s). The related tris(pyrazolyl)methane (tpzm) ligands (e.g. L1′ in Figure 1), on the other hand, have an identical framework to the tpzb ligands but contain a carbon atom instead of the boron atom of tpzb and hence act as neutral ligands. The tpzb and tpzm ligands with identical side chains are therefore expected to have different nucleophilicity and different electron donating properties to metal centers due to their different overall charges.[12]

In contrast, bis(pyrazolyl)methane (bpzm) ligands (e.g. L1′′ in Figure 1) act as neutral bidentate ligands and many complexes containing these ligands have been synthesized.[13–21] In comparison with tpzb, it is interesting to investigate how the structures and properties of complexes are influenced by the different number of coordinating nitrogen donor atoms. Thus, whereas the $Cu^{I}CO$ complex with L1′ is mononuclear, the analogous complex with L1′′ is binuclear with one bridging ClO_4^- anion.[12,20] In addition, the ^{31}P NMR spectrum of the $Cu^{I}PPh_3$ complex of L1′′ shows a narrower signal than that of the corresponding complex with L1′.[20] These differences between tpzm (N3 donor set) and bpzm (N2 donor set) have led to renewed interest in their complexes.

[a] Department of Chemistry, Graduate School of Pure and Applied Sciences, University of Tsukuba, Tsukuba 305-8571, Japan
Fax: +81-29-853-6503
E-mail: kiyoshif@chem.tsukuba.ac.jp

Supporting information for this article is available on the WWW under http://dx.doi.org/10.1002/ejic.200900395.

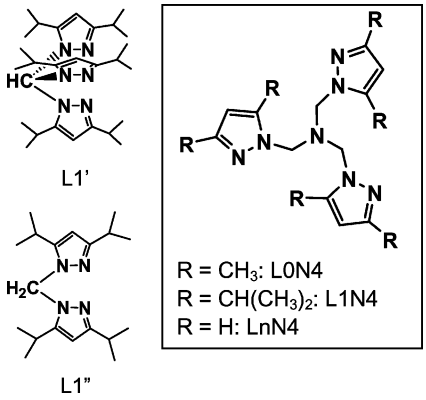

Figure 1. Ligands discussed in this work.

Herein we focus on neutral N4 tripodal tetradentate tris(pyrazol-1-ylmethyl)amine ligands in order to gain more insights into the influence of the number of nitrogen donors on the structures, properties, and reactivity of copper complexes. Various copper complexes with N4 tripodal tetradentate ligands, such as tris{(2-pyridyl)methyl}amine (tpa) and derivatives, have been reported as model compounds of metalloproteins. In the most famous example, Karlin and co-workers reported the structure of the "end-on μ-peroxo" Cu_2O_2 complex $[\{Cu^{II}(tpa)\}_2(O_2)](ClO_4)_2$ and its reactivity.[22,23] Some copper-dioxygen complexes were subsequently also structurally characterized.[22–27] The reactivity of N4-type copper(I) complexes toward other external substrates such as CO and PPh_3 as well as O_2 has also been investigated.[28–31] In addition, many reports have been published concerning N4-type copper(II) complexes with different anions such as Cl^- and N_3^-.[32–37]

In order to investigate the influence of the number of nitrogen donors on the structures, properties, and reactivity, copper complexes containing tris(3,5-dimethylpyrazol-1-ylmethyl)amine[38] (L0N4 in Figure 1) and tris(3,5-diisopropylpyrazol-1-ylmethyl)amine (L1N4 in Figure 1) as pyrazole-containing neutral tetradentate ligands were synthesized in this work and their structures determined by X-ray crystallography. To date, only the crystal structure of the copper(II) azido complex $[Cu(L0N4)(N_3)](ClO_4)$ has been reported.[35] The copper(II) chlorido complexes $[Cu^{II}(L0N4)Cl_2]$ (**1**) and $[Cu^{II}(L1N4)Cl_2]$ (**2**), the copper(II) nitrato complexes $[Cu^{II}(L0N4)(NO_3)](NO_3)$ (**3**) and $[Cu^{II}(L1N4)(NO_3)](NO_3)$ (**4**), the copper(II) sulfato complexes $[Cu^{II}(L0N4)(SO_4)]$ (**5**) and $[Cu^{II}(L1N4)(SO_4)]$ (**6**), and the copper(I) complexes $[Cu^{I}(L0N4)](PF_6)$ (**7**) and $[Cu^{I}(L0N4)(PPh_3)](ClO_4)$ (**8**) containing the neutral tetradentate nitrogen-containing ligands L0N4 and L1N4 were therefore systematically synthesized. All the copper(II) complexes were characterized by IR/far-IR, ESR, and UV/Vis spectroscopy and compared with copper(II) complexes ligated by N2, N3, and analogous N4-type ligands. In addition, we report the reactivity of the copper(I) complexes **7** and **8** toward PPh_3, CO, and O_2. In view of the expected lower reactivity of copper(I) complexes ligated by L1N4, copper(I) complexes were only synthesized for L0N4. Furthermore, the tris(pyrazol-1-ylmethyl)amine ligand[39] (LnN4 in Figure 1) was only used for reactivity studies towards O_2. To the best of our knowledge, no structural determinations of copper complexes with LnN4 and L1N4 have been reported to date. The properties and reactivities of the synthesized copper(I) complexes were investigated by IR/far-IR, UV/Vis, and NMR spectroscopy, and compared with copper(I) complexes containing N2, N3, and analogous N4-type ligands. From these systematic results, some interesting effects concerning the number of nitrogen donors on the structures, properties, and reactivities of the complexes are elucidated.

Results and Discussion

Syntheses

Ligands L0N4 and LnN4 were synthesized following the procedure reported by Driessen,[38,39] whereas L1N4 was synthesized by a modified version of this procedure (see Scheme 1).

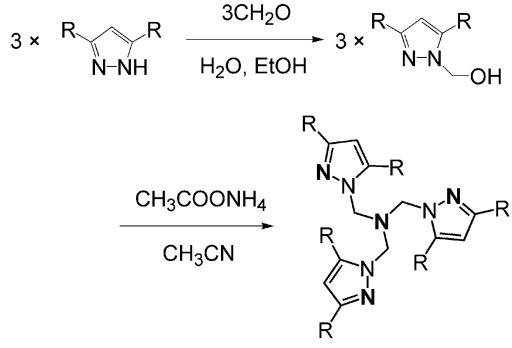

Scheme 1. Synthesis of N4-type ligands.

To avoid reaction with atmospheric dioxygen and moisture, all complexes were synthesized under argon [the copper(I) complexes were prepared in a glovebox]. As shown in Scheme 2, the copper(II) chlorido complexes $[Cu(L0N4)Cl_2]$ (**1**) and $[Cu(L1N4)Cl_2]$ (**2**), the copper(II) nitrato complexes $[Cu(L0N4)(NO_3)](NO_3)$ (**3**) and $[Cu(L1N4)(NO_3)](NO_3)$ (**4**), and the copper(II) sulfato complexes $[Cu(L0N4)(SO_4)]$ (**5**) and $[Cu(L1N4)(SO_4)]$ (**6**) were obtained by treating ligand L0N4 or L1N4 with the corresponding copper(II) salts. Likewise, the copper(I) complex $[Cu(L0N4)](PF_6)$ (**7**) was synthesized by treating $[Cu(CH_3CN)_4](PF_6)$ with L0N4 (see Scheme 3). The smaller ligand L0N4 was used to prepare copper(I) complexes due to the expected lower reactivity of copper(I) precursors with L1N4, and the smallest ligand LnN4 was also used in addition to L0N4 to investigate the reactivity of the copper(I) complexes toward dioxygen. Single crystals could not be obtained for complex **7**, therefore its structure was inferred from other spectroscopic data and elemental analysis. $[Cu(L0N4)(PPh_3)](ClO_4)$ (**8**) was obtained upon treatment of **7** with PPh_3 and $NaClO_4$.

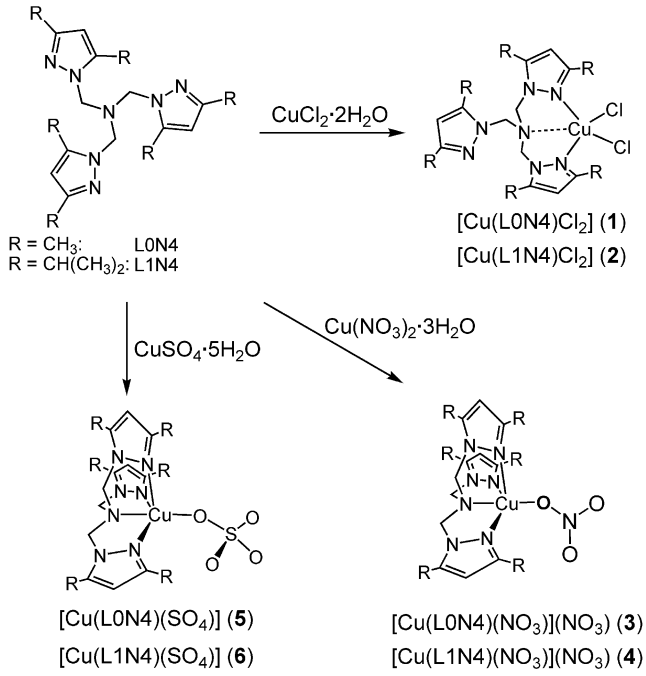

Scheme 2. Synthesis of copper(II) complexes of L0N4 and L1N4.

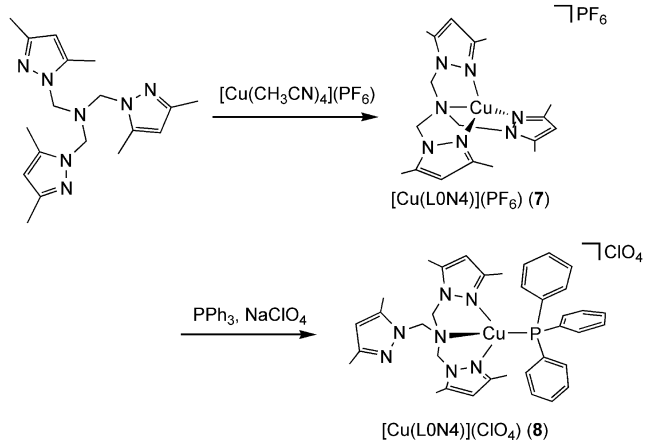

Scheme 3. Synthesis of copper(I) complexes with L0N4.

Structures

The previously reported N4-type ligand L0N4 and the novel ligand L1N4 were obtained as single crystals and their structures determined by X-ray crystallography. Perspective drawings of L0N4 and L1N4 are shown in Figures 2 and S1, respectively. Despite their different substituents, the average bond lengths and angles in L0N4 and L1N4 are almost identical, which suggests that the substituents at the 3- and 5-positions of the pyrazolyl rings do not affect their structures. However, important differences in certain bond lengths and angles are observed in the copper complexes of these ligands due to the steric hindrance of the substituents in the complexes. In other words, the second coordination sphere effects of the ligands are reflected in the resulting complex structures. Moreover, the bond angles around the tertiary amine nitrogen (N41) are almost 109°, thus indicating a tetrahedral geometry around N41.

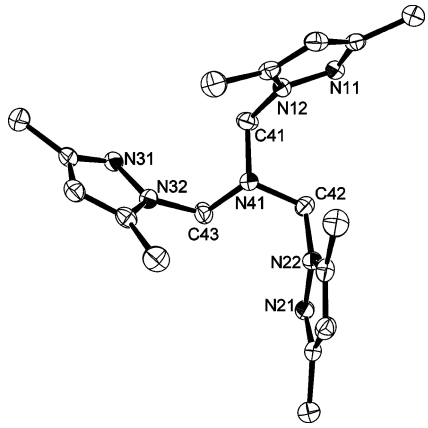

Figure 2. Molecular structure of L0N4 showing 50% thermal ellipsoids and the atom labeling scheme. Hydrogen atoms have been omitted for clarity. Selected bond lengths [Å] and angles [°] for L0N4: N41–C41 1.471(3), N41–C42 1.471(3), N41–C43 1.471(3), C41–N12 1.451(3), C42–N22 1.455(3), C43–N32 1.457(3); C41–N41–C42 110.2(2), C42–N41–C43 110.2(2), C43–N41–C41 110.3(3), N12–C41–N41 110.4(2), N22–C42–N41 110.3(2), N32–C43–N41 110.1(2). For L1N4: N41–C41 1.460(3), N41–C42 1.474(3), N41–C43 1.473(4), C41–N12 1.452(4), C42–N22 1.447(3), C43–N32 1.449(3); C41–N41–C42 110.3(2), C42–N41–C43 110.2(2), C43–N41–C41 109.9(2), N12–C41–N41 113.0(2), N22–C42–N41 112.8(2), N32–C43–N41 112.3(2).

Complexes **1**–**6** and **8** were obtained as single crystals and their structures determined by X-ray crystallography. The molecular structures of these complexes, with selected bond lengths and angles in the respective figure captions, are shown in Figures 3, 4, 5, 6 and S2–S4, respectively. Selected structural parameters for the synthesized and reported complexes are listed in Tables 1, 2, 3, and 4. Chlorido and sulfato complexes **1**, **2**, **5**, and **6** are neutral and the oxidation state of each copper ion is +2. Nitrato complexes **3** and **4** are cationic, with one nitrate ion as counterion, and the oxidation state of each copper ion is also +2. The oxidation state of copper is +1 in the triphenylphosphane complex **8** due to the presence of only one ClO_4^- anion. The distances from copper to an axial nitrogen atom (labeled N21 in this work) in the four complexes **3**–**6** are longer than those between copper(II) ions and the other two equatorial pyrazolyl nitrogen atoms (N11 and N31 in this work), thus suggesting the presence of a Jahn–Teller effect.

The L0N4 and L1N4 ligands in the copper(II) chlorido complexes **1** and **2** bind the copper(II) ions as tridentate ligands, with one pyrazolyl arm of each ligand remaining uncoordinated. Complexes **1** and **2** therefore consist of a copper(II) ion surrounded by three nitrogen atoms from the N4-type ligand and two chloride anions. The observed differences due to steric interactions between the two ligands are small. In terms of the trigonality index for five-coordinate environments (τ) introduced by Addison et al. [$\tau = (\alpha - \beta)/60°$, where α and β are the largest angles ($\alpha \geq \beta$) around

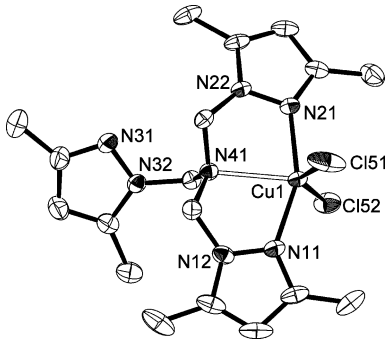

Figure 3. Molecular structure of [Cu(L0N4)Cl_2] (**1**) showing 50% thermal ellipsoids and the atom labeling scheme. Hydrogen atoms have been omitted for clarity. Selected bond lengths [Å] and angles [°] for **1**: Cu1–N11 1.991(2), Cu1–N21 1.995(2), Cu1···N31 5.253(2), Cu1–N41 2.351(2), Cu1–Cl51 2.2645(9), Cu1–Cl52 2.2850(7); N11–Cu1–N21 156.19(9), N11–Cu1–N41 77.89(8), N11–Cu1–Cl51 93.55(6), N11–Cu1–Cl52 94.38(6), N21–Cu1–N41 78.48(8), N21–Cu1–Cl51 93.04(6), N21–Cu1–Cl52 95.15(6), N41–Cu1–Cl51 112.31(5), N41–Cu1–Cl52 107.61(5), Cl51–Cu1–Cl52 140.08(3). For **2**: Cu1–N11 1.970(3), Cu1–N21 1.984(3), Cu1···N31 5.202(4), Cu1–N41 2.314(3), Cu1–Cl51 2.2807(12), Cu1–Cl52 2.2986(15); N11–Cu1–N21 157.81(13), N11–Cu1–N41 79.07(12), N11–Cu1–Cl51 95.57(10), N11–Cu1–Cl52 90.57(12), N21–Cu1–N41 78.78(13), N21–Cu1–Cl51 96.00(11), N21–Cu1–Cl52 92.77(14), N41–Cu1–Cl51 117.51(10), N41–Cu1–Cl52 102.77(10), Cl51–Cu1–Cl52 139.71(4).

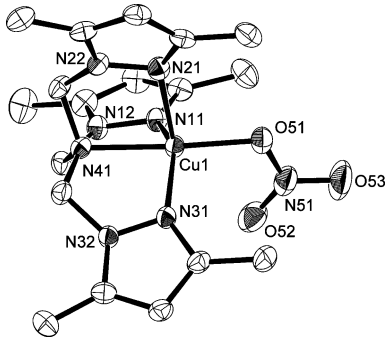

Figure 4. Molecular structure of the cation part of [Cu(L0N4)(NO_3)](NO_3) (**3**) showing 50% thermal ellipsoids and the atom labeling scheme. Hydrogen atoms have been omitted for clarity. Selected bond lengths [Å] and angles [°] for **3**: Cu1–N11 2.014(2), Cu1–N21 2.213(3), Cu1–N31 2.008(2), Cu1–N41 2.101(2), Cu1–O51 1.958(2), Cu1···O52 2.754(3); N11–Cu1–N21 106.99(11), N11–Cu1–N31 141.49(12), N11–Cu1–N41 80.79(10), N11–Cu1–O51 98.48(10), N21–Cu1–N31 103.99(12), N21–Cu1–N41 80.04(11), N21–Cu1–O51 97.24(11), N31–Cu1–N41 82.62(9), N31–Cu1–O51 99.74(9), N41–Cu1–O51 176.79(10). For **4**: Cu1–N11 2.008(2), Cu1–N21 2.242(2), Cu1–N31 2.0079(19), Cu1–N41 2.097(2), Cu1–O51 1.970(2), Cu1···O52 2.604(2); N11–Cu1–N21 97.80(8), N11–Cu1–N31 160.72(9), N11–Cu1–N41 81.62(8), N11–Cu1–O51 97.12(8), N21–Cu1–N31 88.56(8), N21–Cu1–N41 82.60(8), N21–Cu1–O51 112.16(9), N31–Cu1–N41 81.18(8), N31–Cu1–O51 97.28(8), N41–Cu1–O51 165.17(9).

a five-coordinate metal center; τ is zero for a perfect square pyramid and one for a trigonal bipyramid],[40] the coordination geometries of both complexes are distorted square pyramids (τ = 0.27 for **1** and 0.30 for **2**; Table 1). This is attributed to the fact that the steric repulsion between the substituents of the two ligated pyrazolyl arms and the two

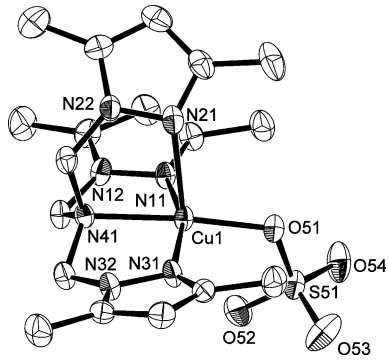

Figure 5. Molecular structure of [Cu(L0N4)(SO_4)] (**5**) showing 50% thermal ellipsoids and the atom labeling scheme. Hydrogen atoms have been omitted for clarity. Selected bond lengths [Å] and angles [°] for **5**: Cu1–N11 2.017(3), Cu1–N21 2.305(3), Cu1–N31 1.996(4), Cu1–N41 2.105(3), Cu1–O51 1.926(3); N11–Cu1–N21 86.90(14), N11–Cu1–N31 160.01(15), N11–Cu1–N41 81.32(14), N11–Cu1–O51 98.69(14), N21–Cu1–N31 99.85(14), N21–Cu1–N41 81.37(13), N21–Cu1–O51 104.09(13), N31–Cu1–N41 81.14(14), N31–Cu1–O51 97.86(14), N41–Cu1–O51 174.53(12). For **6**: Cu1–N11 2.002(4), Cu1–N21 2.242(4), Cu1–N31 2.011(4), Cu1–N41 2.123(4), Cu1–O51 1.928(4); N11–Cu1–N21 87.90(17), N11–Cu1–N31 159.46(18), N11–Cu1–N41 82.49(17), N11–Cu1–O51 98.53(18), N21–Cu1–N31 98.44(18), N21–Cu1–N41 79.28(17), N21–Cu1–O51 109.09(17), N31–Cu1–N41 79.56(16), N31–Cu1–O51 97.80(16), N41–Cu1–O51 171.57(16).

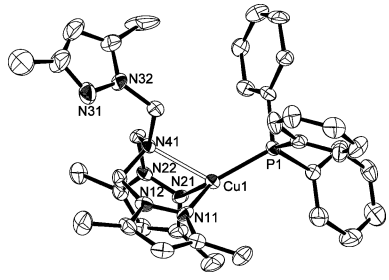

Figure 6. Molecular structure of the cation part of [Cu(L0N4)(PPh_3)](ClO_4) (**8**) showing 50% thermal ellipsoids and the atom labeling scheme. Two crystallographically independent molecules are present, whose structural features are essentially identical. Molecule 1 is presented here. Hydrogen atoms have been omitted for clarity. Selected bond lengths [Å] and angles [°]: Cu1–N11 2.012(6), Cu1–N21 2.033(7), Cu1–N41 2.313(7), Cu1–P1 2.171(2); N11–Cu1–N21 107.3(2), N11–Cu1–N41 78.0(2), N11–Cu1–P1 128.3(2), N21–Cu1–N41 76.4(2), N21–Cu1–P1 123.2(2), N41–Cu1–P1 121.78(19); Cu2–N51 1.984(6), Cu2–N61 2.026(7), Cu2–N81 2.364(7), Cu2–P2 2.166(2); N51–Cu2–N61 105.0(3), N51–Cu2–N81 77.8(2), N51–Cu2–P2 128.6(2), N61–Cu2–N81 76.4(2), N61–Cu2–P2 124.8(2), N81–Cu2–P2 122.35(19).

chlorido ligands is very small because each position is distant enough in this structure. The axial position is occupied by the tertiary amine nitrogen (N41), which contrasts with the situation in other complexes. The coordination geometries of complexes **1** and **2** are similar to those of [Cu(L1′′)-Cl_2][20,41] and [Cu(L1′)Cl_2],[42] which also have two bound chloride anions. The average Cu–Cl bond lengths in the three complexes [Cu(L1′′)Cl_2], [Cu(L1′)Cl_2], and **2**, which have the same isopropyl substituents on the pyrazolyl rings, are 2.22,[20,41] 2.26,[42] and 2.29 Å, respectively. This increase seems to be due to the different number of coordinat-

Table 1. Selected structural parameters for copper(II) chlorido complexes with N2-, N3-, and N4-type ligands.

	Cu–$N_{pz/pyr}$ (av) [Å]	Cu–Cl (av) [Å]	Cl–Cu–Cl [°]	τ[40]	Coordination type	Ref.
[Cu(L0N4)Cl_2] (**1**)	1.993	2.275	140.08(3)	0.27	N3Cl2	this work
[Cu(L1N4)Cl_2] (**2**)	1.977	2.290	139.71(4)	0.30	N3Cl2	this work
[Cu(Me_3tpa)Cl_2]	2.015	2.333	131.4(1)	0.53	N3Cl2	[34]
[Cu(tpa)Cl](PF_6)	2.140	2.233(2)		1.01	N4Cl	[32]
[Cu(Me_1tpa)Cl](ClO_4)	2.105	2.249(3)		0.16	N4Cl	[34]
[Cu(Me_2tpa)Cl](ClO_4)	2.090	2.253(4)		0.07	N4Cl	[34]
[Cu(Me_3tpa)Cl](ClO_4)	2.081	2.240(2)		0.43	N4Cl	[34]
[Cu(pmea)Cl](ClO_4)[a]	2.092	2.278		0.12	N4Cl	[29]
[Cu(pmap)Cl](ClO_4)[b]	2.098	2.2690(12)		0.08	N4Cl	[29]
[Cu(tepa)Cl](PF_6)[c]	2.109	2.289(1)		0.19	N4Cl	[32]
[Cu(bpqa)Cl](PF_6)[d]	2.114	2.257(2)		0.16	N4Cl	[33]
[Cu(tmqa)Cl](PF_6)[e]	2.056	2.244(2)		0.06	N4Cl	[33]
[Cu(L1′′)Cl_2]	1.990	2.224	103.2		N2Cl2	[20,41]
[Cu(L1′)Cl_2]	2.140	2.258	93.38(6)	0.12	N3Cl2	[42]

[a] pmea = bis[(2-pyridyl)methyl]-2-(2-pyridyl)ethylamine. [b] pmap = bis[2-(2-pyridyl)ethyl](2-pyridyl)methylamine. [c] tepa = tris[2-(2-pyridyl)ethyl]amine. [d] bpqa = bis[(2-pyridyl)methyl](2-quinolylmethyl)amine. [e] tmqa = tris[(2-quinolyl)methyl]amine.

Table 2. Selected structural parameters for copper(II) nitrato complexes with N2-, N3-, and N4-type ligands.

	Cu–N_{pz} (av) [Å]	Cu–O (av) [Å]	τ[40]	Coordination type	Ref.
[Cu(L0N4)(η^1-ONO_2)](NO_3) (**3**)	2.078	1.958(2)	0.59	N4O	this work
[Cu(L1N4)(η^1-ONO_2)](NO_3) (**4**)	2.086	1.970(2)	0.07	N4O	this work
[Cu(L1′′)(η^1-ONO_2)$_2$]	1.989	1.992		N2O2	[41,43]
[Cu(L1′)(η^1-ONO_2)$_2$]	2.100	1.955	0.26	N3O2	[42]
[Cu(L2′)(η^2-O_2NO)](ClO_4)[a]	2.078	2.002	0.30	N3O2	[44]

[a] L2′ = tris(3-*tert*-butyl-5-methyl-1-pyrazolyl)methane.

Table 3. Selected structural parameters for copper(II) sulfato complexes with N3- and N4-type ligands.

	Cu–N_{pz} (av) [Å]	Cu–O (av) [Å]	τ[40]	Coordination type	Ref.
[Cu(L0N4)(η^1-OSO_3)] (**5**)	2.106	1.926(3)	0.24	N4O	this work
[Cu(L1N4)(η^1-OSO_3)] (**6**)	2.085	1.928(4)	0.20	N4O	this work
[Cu(L1′)(η^2-O_2SO_2)]	2.083	1.964	0.23	N3O2	[45]

Table 4. Selected structural parameters for copper(I) triphenylphosphane complexes with N2-, N3-, and N4-type ligands.

	Cu–$N_{pz/pyr}$ (av) [Å]	Cu–P (av) [Å]	P–Cu–$N_{pz/pyr}$ (av) [°]	Coordination type	Ref.
[Cu(L0N4)(PPh_3)](ClO_4) (**8**)	2.023	2.171(2)	125.8	N3P	this work
[Cu(tpa)(PPh_3)](PF_6)	2.071	2.194(2)	121.7	N3P	[23]
[Cu(bqpa)(PPh_3)](ClO_4)[a]	2.08	2.200(9)	125.0	N3P	[28]
[Cu(L0′′)(PPh_3)](ClO_4)[b]	2.019	2.171	131.2	N2P	[16]
[Cu(L1′′)(PPh_3)](ClO_4)	2.008	2.174(2)	131.9	N2P	[20]
[Cu(L1′′)(PPh_3)](PF_6)	2.006	2.1726(12)	132.3	N2P	[20]
[Cu(L1′)(PPh_3)](ClO_4)	2.085	2.166(6)	126.0	N3P	[20]

[a] bqpa = bis(2-pyridylmethyl)(2-quinolylmethyl)amine. [b] L0′′ = bis(3,5-dimethyl-1-pyrazolyl)methane.

ing nitrogen atoms and the presence of an interacting tertiary amine nitrogen donor in complex **2**. As can be seen from Table 1, many copper(II) chlorido complexes with N4-type ligands have been reported. Most of these structures, however, have N4Cl ligand donor sets, and the N3Cl2-type coordination in complexes **1** and **2** is very rare. The ligands in N4Cl-type complexes have small or no substituents near the copper(II) ion, which means that complexes with bulkier substituents tend to belong to the N3Cl2 class. Moreover, the N(tertiary amine nitrogen)–Cu bond lengths are different. Thus, the Cu1–N41 bond lengths are 2.351(2) Å for **1** and 2.314(3) Å for **2**, whereas the Cu–N1(tertiary amine nitrogen) bond length in [Cu(Me_3tpa)Cl_2], which is of the same N3Cl2 type, is 2.145(6) Å,[34] thereby indicating very weak interactions between the tertiary amine nitrogens and the copper(II) center in complexes **1** and **2**.

The L0N4 and L1N4ligands in the copper(II) nitrato complexes **3** and **4** bind the copper(II) ions as tetradentate ligands. Complexes **3** and **4** therefore consist of a copper(II) ion surrounded by four nitrogen donor atoms from the N4-type ligand and one oxygen atom from the bound nitrate ion; another nitrate ion is present as a counterion. This coordination geometry differs from the geometries of [Cu(L1′′)(η^1-ONO_2)$_2$][41,43] and [Cu(L1′)(η^1-ONO_2)$_2$],[42] in which two nitrate ions coordinate to the copper(II) ion in a monodentate mode. In addition, it is also different from [Cu(L2′)(η^2-O_2NO)](ClO_4) [L2′ = tris(3-*tert*-butyl-5-methyl-1-pyrazolyl)methane], in which only one nitrate ion

coordinates in a bidentate mode due to the increased bulkiness of the *tert*-butyl group, which does not allow two nitrates to coordinate.[44] Interestingly, the coordination environments of complexes **3** and **4** are different (τ = 0.59 for **3** and 0.07 for **4**), thus indicating different degrees of steric repulsion between the different methyl and isopropyl substituents of the pyrazolyl moieties of the N4-type ligands and the coordinating planar nitrate ion (see Table 2). No N4O-type coordination modes have been reported to date for any type of nitrogen donor ligand in a nitrato complex, therefore the corresponding structural differences cannot be discussed.

The copper(II) ion in sulfato complexes **5** and **6** has a five-coordinate geometry with four Cu–N bonds from the N4-type ligand and one Cu–O bond to the sulfate ion. This coordination geometry differs from that of [Cu(L1′)(η^2-O_2SO_2)],[45] which has two Cu–O bonds to a bidentate sulfate ion (see Table 3). In contrast to the copper(II) nitrato complexes **3** and **4**, the coordination environments of the copper(II) ion in complexes **5** and **6** are similar and correspond to a distorted square pyramidal geometry (τ = 0.24 for **5** and 0.20 for **6**). This is because the tetrapod-shaped sulfate ion is much bulkier than the planar nitrate ion, which means that even **5**, which has only small methyl substituents, cannot have a distorted trigonal bipyramidal geometry.

One pyrazolyl arm of the L0N4 ligand in the copper(I) triphenylphosphane complex **8** remains uncoordinated, as is the case with previously reported analogous complexes with the tpa ligand (see Table 4).[23] This is attributed to the fact that a four-coordinate geometry is generally preferred in copper(I) complexes. The copper(I) ion is placed in a trigonal plane consisting of two pyrazolyl nitrogen atoms from L0N4 and the phosphorus atom of the PPh_3 molecule [sum of angles around the copper(I) ion: 358.7°]. In addition, the copper(I) ion interacts weakly with the tertiary amine nitrogen atom (N41 or N81) of L0N4 in the axial position above the trigonal plane. This is in agreement with the distances between the N2P least-squares plane and the copper(I) ions [0.134(1) Å for Cu1 and 0.148(1) Å of Cu2], both of which show a higher planarity. The previously reported N2-type ligands L0′′ and L1′′ form a trigonal planar geometry in copper(I) triphenylphosphane complexes,[16,20] and the N3-type ligand L1′ shows a tetrahedral geometry.[20] As shown in Table 4, the average Cu–N_{pz} distance in complex **8** (2.023 Å) is almost the same as the average value for the N2-type complexes [Cu(L1′′)(PPh_3)](ClO_4) (2.008 Å)[20] and [Cu(L0′′)(PPh_3)](ClO_4) (2.019 Å)[16] but shorter than that for the N3-type complex [Cu(L1′)(PPh_3)](ClO_4) (2.085 Å).[20] The reason for this trend is that the bulkier pyrazolyl ligands result in a stronger steric repulsion with bulky PPh_3. The average Cu–N_{pz} distances for the complexes with N2- and N4-type ligands, which have two Cu–N_{pz} bonds, are therefore shorter than those with the N3-type ligand which has three Cu–N_{pz} bonds. In the latter case, three pyrazolyl rings of the ligand and three phenyl rings of triphenylphosphane are alternately placed in order to minimize the steric repulsion. Interestingly, the Cu–P bond lengths of the related complexes [Cu(L1′′)(PPh_3)](ClO_4) [2.174(2) Å],[20] [Cu(L0′′)(PPh_3)](ClO_4) (2.171 Å),[16] N4-type complex **8** [2.171(2) Å], and the N3-type complex [Cu(L1′)(PPh_3)](ClO_4) [2.166(6) Å] are almost the same.[20] As was also the case for complexes **1** and **2**, the Cu–N(tertiary nitrogen) bond lengths in complex **8** [2.313(7) Å for Cu1 and 2.364(7) Å for Cu2] are longer than those for [Cu(tpa)(PPh_3)](PF_6) [2.248(6) Å][23] and [Cu(bqpa)(PPh_3)](ClO_4) [2.19(2) Å],[28] which have the same N3P-type ligand environment, thus indicating weaker interactions of the tertiary amine nitrogens with the copper(I) center in **8**.

Properties of Copper(II) Complexes

IR Spectra

No new characteristic bands are observed for the chlorido complexes in the 600–1800 cm^{-1} region, therefore the stretching vibrations of complexes **1** and **2** are almost identical to those of the corresponding ligands.

The assignments of stretching vibrations in the nitrato complexes **3** and **4** are based on those of previously reported nitrato complexes.[41–44,46] Thus, the coordinated nitrate ion shows three N–O stretching bands in the 1000–1500 cm^{-1} region, whereas the nitrate counterion is responsible for the broad peak at 1385 cm^{-1}. As the N–O bond lengths in the literature compounds are almost identical to those in complexes **3** and **4**, the N–O stretching bands should be observed at very similar frequencies. In general, the energy separation between the two highest-frequency N–O stretching bands for monodentate coordination is smaller than that for bidentate coordination if the complexes have a similar coordination mode.[46] Indeed, the ν_5–ν_1 values for monodentate nitrato complexes in an N4O-type (179 cm^{-1} for **3**, 197 cm^{-1} for **4**), N3O2-type {184 cm^{-1} for [Cu(L1′)(η^1-ONO_2)$_2$]}, and N2O2-type ligand environment {231 cm^{-1} for [Cu(L1′′)(η^1-ONO_2)$_2$]} are smaller than those for a symmetric bidentate nitrato complex in an N3O2-type ligand environment {282 cm^{-1} for [Cu(L2′)(η^2-O_2NO)](ClO_4)}.

S–O stretching bands are observed in the 600–1200 cm^{-1} region for sulfato complexes **5** and **6**. Since the S–O bond lengths are almost the same in complexes **5** and **6**, the ν_1, ν_3, and ν_4 S–O stretching bands should be observed at almost the same frequency. In general, each ν_3 and ν_4 mode splits into two bands in monodentate sulfato complexes, whereas three bands are observed in bidentate ones as the symmetry-lowering which results upon coordination is different for monodentate and bidentate complexes.[46] In fact, bands ν_3 and ν_4 in **5** and **6** are split into two features whereas bands ν_3 and ν_4 in [Cu(L1′)(η^2-O_2SO_2)] split into three separate bands, thereby reflecting the different coordination modes (monodentate and bidentate) in these complexes.[45]

Far-IR Spectra

In this work, far-IR spectra were recorded as Nujol mulls as all the synthesized copper(II) complexes changed color

upon mixing with CsI. A comparison of L0N4 with L1N4 complexes **1**–**6** allowed the bands resulting from Cu–X stretching vibrations (X = Cl for **1** and **2**, O for **3**–**6**) to be identified at very similar positions as a result of the similar bond lengths. The stretching bands were assigned by comparison to those of reported complexes.[20,41–46]

The coordinating chloride ion in complexes **1** and **2** shows a broad peak for ν(Cu–Cl) at 310 cm^{-1} for **1** and 309 cm^{-1} for **2**. The Cu–Cl stretching bands of [Cu(L1′′)-Cl_2] (315 cm^{-1})[20] and [Cu(L1′)Cl_2] (295 cm^{-1})[42,43] are also observed around 300 cm^{-1} because of the similar Cu–Cl bond lengths with respect to **1** and **2**. The coordinating nitrate ions in complexes **3** and **4** show peaks for ν(Cu–O) at 324 and 333 cm^{-1}, respectively. The Cu–O stretching frequencies of [Cu(L1′′)$(NO_3)_2$] (323 cm^{-1})[41] and [Cu(L1′)-$(NO_3)_2$] (327 cm^{-1})[42,43] are similar to those of **3** and **4** because the coordination modes of the nitrate ions are similar in these four complexes (nearly asymmetric monodentate). The coordinating sulfate ion in complexes **5** and **6** shows peaks for ν_2(S–O) and ν(Cu–O). The ν_2(S–O) peaks are observed at 449 and 433 cm^{-1} for **5** and **6**, respectively, and the ν(Cu–O) peaks are observed at 299 and 309 cm^{-1}, respectively. In [Cu(L1′)(SO_4)],[45] however, these two peaks [ν_2(S–O) at 464 cm^{-1} and ν(Cu–O) at 322 cm^{-1}] are observed at higher frequency than for **5** and **6** because of the different coordination mode of the sulfate ions (monodentate and bidentate).

UV/Vis Spectra

The UV/Vis spectra of complexes **1**–**6** were recorded in dichloromethane solution. In general, copper(II) complexes containing tripodal tetradentate ligands can have a square-pyramidal or a trigonal-bipyramidal coordination mode, with the d–d absorption bands of those copper(II) complexes with a square-pyramidal configuration being shifted to higher energy than those with a trigonal-bipyramidal configuration.[47]

The d–d transition bands in chlorido complexes **1** (τ = 0.27) and **2** (τ = 0.30) are observed at 858 and 847 nm, respectively. This similarity in energy is due to the almost identical coordination structure in these compounds. In addition, two ligand-to-metal charge transfer (LMCT) transition bands from chloride to the copper(II) ion are observed around 350 and 280 nm in both complexes **1** and **2**. It is unclear why the absorption coefficients of **2** are higher than those of **1** in the CT region. The d–d transition bands of complexes **1** and **2** are observed at different energies to those in other N2- and N3-type chlorido complexes such as [Cu(L1′)Cl_2] (756 nm, τ = 0.12) and [Cu(L1′′)Cl_2] (911 nm, four-coordinate structure).[20,41,42] It seems likely that the energy gap between the d orbitals in these complexes is different because of the different structural distortions. The d–d transition bands in nitrato complexes **3** and **4** are found at 756 and 748 nm, respectively. It is surprising that these two bands are observed at similar wavelengths despite their different coordination geometries (τ = 0.59 for **3** and 0.07 for **4**). In addition, [Cu(L1′′)$(NO_3)_2$] (741 nm, square planar)[41] and [Cu(L1′)$(NO_3)_2$] (730 nm, τ = 0.26: square pyramidal)[42] also show d–d transition bands at similar wavelengths to those for **3** and **4**. These results appear to show that the structure of **3** changes to nearly square pyramidal in solution. This is also supported by ESR spectroscopy (see below).

The LMCT transition bands from nitrate to the copper(II) ion in **3** and **4** are observed at 312 and 302 nm, respectively. The absorption coefficients of the LMCT bands of the N4-type nitrato complexes **3** and **4** are weaker than those of N2- and N3-type ones. This is attributed to the fact that the N4-type complexes are coordinated by one nitrate ion whereas N2- and N3-type complexes have two coordinating nitrate ions.

The sulfato complexes **5** and **6** show similar spectral patterns, with d–d transition bands at 709 and 720 nm, respectively. This is consistent with their similar coordination geometries (τ = 0.24 for **5** and 0.20 for **6**). However, these energies are different from those of [Cu(L1′)(SO_4)] (679 nm).[45] This can be explained by the different binding modes of the sulfate ion, which is monodentate in complexes **5** and **6** and bidentate in [Cu(L1′)(SO_4)]. The absorption bands in **5** (286 nm) and **6** (275 nm) corresponding to the LMCT transitions are observed at slightly different wavelengths. This seems to be related to the different Cu–O51–S–O53 torsion angles in **5** (10.7°) and **6** (27.2°). In addition, these LMCT transition bands in complexes **5** and **6** are observed at higher energy than that in [Cu(L1′)(SO_4)] (294 nm), where the sulfate ion is bidentate.

ESR Spectra

Since $g_{\|} > g_{\perp} > 2.0023$ for all complexes **1**–**6**, the unpaired electron of the copper(II) ion resides in the $d_{x^2-y^2}$ orbital in all cases.[48] In other words, the copper(II) ion has a five-coordinate square-pyramidal geometry in solution, as determined above from the UV/Vis spectra. A comparison with other complexes shows that the ESR spectrum of [Cu(L1′′)Cl_2], which has a distorted tetrahedral structure, shows a rhombic signal.[20,43] In general, $A_{\|}$ values for complexes with a square-pyramidal or a trigonal-bipyramidal structure are smaller than those of complexes with a square planar geometry around the copper ion.[48] The $A_{\|}$ values of all the new complexes **1**–**6** are smaller than the $A_{\|}$ value of [Cu(L1′′)$(NO_3)_2$], which has a square-planar structure. The electronic absorption and ESR spectra therefore confirm that the coordination geometry of complex **3** determined by X-ray crystallography is not maintained in solution.

Properties of Copper(I) Complexes

IR and Far-IR Spectra

The IR and far-IR spectra of copper(I) complexes **7** and **8** were measured as KBr and CsI pellets, respectively. In the case of **7**, the ν(P–F) and δ(F–P–F) bands derived from the PF_6^- counterion are observed at 842 and 559 cm^{-1}, respectively. In addition, the ν(Cu–N) vibration of the coordinating pyrazolyl arms is observed at 292 cm^{-1}.[20,46] In the tri-

phenylphosphane complex **8**, the ν(Cl–O) and δ(O–Cl–O) bands derived from the ClO_4^- counterion are observed at 1095 and 624 cm^{-1}, respectively. Complex **8** also shows strong bands at 531 and 499 cm^{-1}, which were assigned to Cu–P stretching and C–P–C bending vibrations.[20,49,50] Unfortunately, the ν(Cu–P) band could not be identified from the spectra, probably because it is overlapped by absorptions due to the pyrazolyl ring system.[20] The ν(Cu–N) band for complex **8** is observed at 276 cm^{-1}. These bands are also observed in the other complexes.

NMR Spectra

The ^1H and ^{13}C NMR spectra of complexes **7** and **8** were measured, and the appropriate signals for the protons and carbon atoms of the tetradentate nitrogen-containing ligands were observed. As single crystals of **7** could not be obtained, the coordination mode of L0N4 to copper(I) ion was determined on the basis of the ^1H NMR spectrum and elemental analysis. The clear downfield shifts of the pyrazolyl ring protons (see Figure 7) indicate that L0N4 coordinates to the copper(I) ion in complex **7**. In addition, no peaks which can be assigned to protons from coordinated acetonitrile are observed, therefore acetonitrile does not coordinate to the copper(I) center. This coordination mode is also supported by satisfactory elemental analysis of complex **7**. As can be seen from Table 5, complexes with bound acetonitrile ligands tend to form when the N4-type ligand has substituents adjacent to the copper(I) ion, as in L0N4.[51]

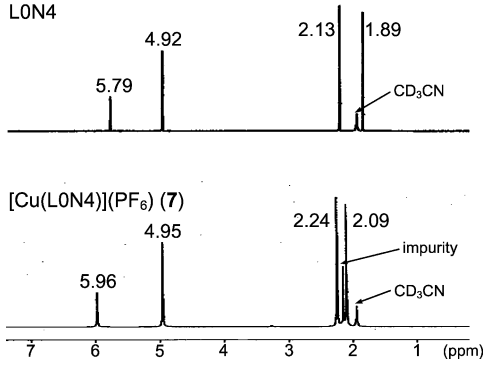

Figure 7. ^1H NMR spectra of L0N4 (top) and **7** (bottom).

Table 5. ^1H NMR chemical shifts of coordinated acetonitrile ligands in copper(I) complexes.

	δ(^1H) [ppm]	Ref.
[Cu(L0N4)](PF_6) (**7**)		this work
[Cu(tpa)(CH_3CN)](PF_6)	2.01	[23]
[Cu(tpa)(CH_3CN)](ClO_4)	2.00	[23]
[Cu(Me_1tpa)](ClO_4)		[51]
[Cu(Me_2tpa)](PF_6)		[51]
[Cu(Me_3tpa)](BF_4)		[51]
[Cu(L1′′)(CH_3CN)](PF_6)	2.31	[20]
[Cu(L1′)(CH_3CN)](PF_6)	2.34	[12]
[Cu(L1′)(CH_3CN)](ClO_4)	2.29	[12]

The ^{31}P NMR spectrum of the copper(I) triphenylphosphane complex **8** shows a single resonance for PPh_3, as shown in Figure 8. Table 6 lists the ^{31}P NMR chemical shifts for this and other related triphenylphosphane complexes. All these signals appear downfield of free triphenylphosphane, thereby indicating a decreased shielding due to the presence of the metal, as expected for a σ-donor ligand like phosphane. The ^{31}P NMR chemical shift of PPh_3 in complex **8** is δ = 3.75 ppm. The related copper(I) triphenylphosphane complexes [Cu(L1′′)(PPh_3)](ClO_4) and [Cu(L1′′)(PPh_3)](PF_6) are trigonal planar with similar structures, which is consistent with their almost identical chemical shifts of δ = 12.11 and 12.20 ppm, respectively.[20] Moreover, the chemical shift of PPh_3 in [Cu(L1′)(PPh_3)](ClO_4), which has a tetrahedral geometry, is δ = 13.79 ppm.[20] These chemical-shift differences between [Cu(L1′′)(PPh_3)](ClO_4) {or [Cu(L1′′)(PPh_3)](PF_6)} and [Cu(L1′)(PPh_3)](ClO_4) support the difference in Cu–P interactions in these complexes. Thus, the somewhat larger chemical shift for [Cu(L1′)(PPh_3)](ClO_4) indicates that PPh_3 is a stronger donor to the copper center in this complex, which is consistent with the shorter Cu–P bond length in this case (Table 6). Interestingly, the chemical shift of complex **8** is much smaller despite the similar Cu–P bond lengths in **8** and other complexes. It therefore seems that the Cu–P bond length in the crystal structure of complex **8** is not maintained in solution at room temperature. In fact, The ^1H NMR spectrum of complex **8** in CD_3CN solution indicates that the protons of the three pyrazolyl arms of L0N4 are equivalent despite one arm being uncoordinated in the crystal structure (Figure 6). According to the literature, differences in signal width are due to the inherent instability of the complexes in solution[13] and therefore correlate with the bond strength of the Cu–P bond in solution.[20,26,52,53] The half width of the signal in complex **8** (270.4 Hz) is similar to that of [Cu(L1′)(PPh_3)](ClO_4) (323.5 Hz), which is probably due to the fact that these compounds show similar N_3P coordination modes around

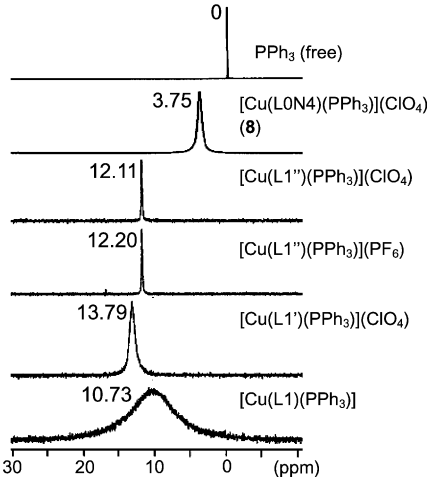

Figure 8. ^{31}P NMR spectra of copper(I) triphenylphosphane complexes in the PPh_3 resonance region. ^{31}P chemical shifts are referenced relative to an external standard of PPh_3 (δ = 0 ppm, top).

Table 6. ^{31}P NMR chemical shifts of coordinated triphenylphosphane in copper(I) triphenylphosphane complexes.

	$\delta(^{31}P)$ [ppm]	Cu–P [Å]	Half width [Hz]	Ref.
[Cu(L0N4)(PPh$_3$)](ClO$_4$) (**8**)	3.75	2.171(2)	270.4	this work
[Cu(L1′′)(PPh$_3$)](ClO$_4$)	12.11	2.173(2)	31.5	[20]
[Cu(L1′′)(PPh$_3$)](PF$_6$)	12.20	2.173(1)	30.5	[20]
[Cu(L1′)(PPh$_3$)](ClO$_4$)	13.79	2.160(4)	323.5	[20]
[Cu(L1)(PPh$_3$)]	10.73	2.164(1)	1626.5	[20,52,53]

the copper(I) ion. It therefore appears that the stability of the Cu–P bond in complex **8** is similar to that in [Cu(L1′)(PPh$_3$)](ClO$_4$).

Reactivity of Copper(I) Complexes

The reactivity of **7** toward PPh$_3$, CO, and O$_2$ (Scheme 4) was investigated and compared with that of [Cu(L1′)(CH$_3$CN)](ClO$_4$) (Scheme 5) and [{Cu(L1′′)}$_2$](ClO$_4$)$_2$ (Scheme 6).[12,20]

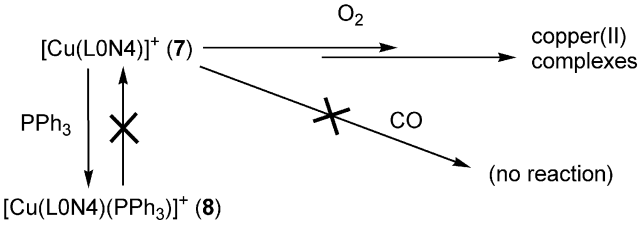

Scheme 4. Reactivity of copper(I) complexes containing L0N4.

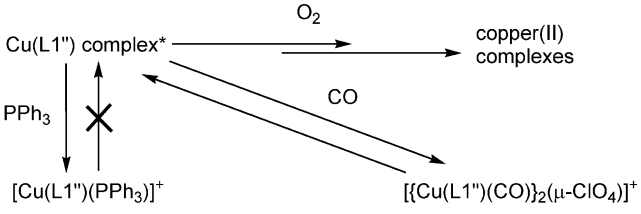

Scheme 5. Reactivity of copper(I) complexes containing L1′′ {*Cu(L1′′) = [Cu$_2$(L1′′)$_2$](ClO$_4$)$_2$ or [Cu(L1′′)$_2$](ClO$_4$)}.[20]

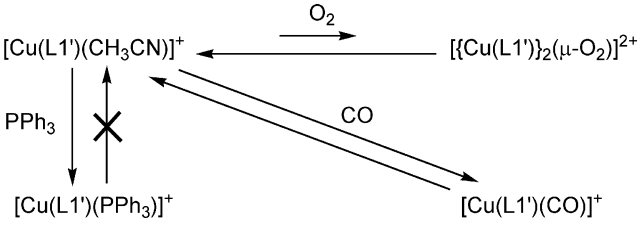

Scheme 6. Reactivity of copper(I) complexes containing L1′.[20]

The treatment of **7** with one equivalent of PPh$_3$ resulted in rapid formation of the triphenylphosphane complex **8**. Since phosphanes are strong σ-donor ligands to copper(I), a distorted four-coordinate copper(I) complex, with L0N4 acting as a tridentate ligand, is obtained. Unfortunately, it was unclear from the far-IR spectrum whether PPh$_3$ coordinates or not, as discussed previously.[20] This problem was solved by ^{31}P NMR spectroscopy (Figure 8), which shows distinct ^{31}P chemical shifts in complex **8** compared to free PPh$_3$. In addition, the reverse reaction was investigated for comparison. As might be expected, the ^{31}P and ^{1}H NMR spectra confirmed that complex **8** does not react back to complex **7** upon stirring in acetonitrile for three days.

After treatment of complex **7** with CO, the solvent was removed under reduced pressure and the IR spectrum of the crude product measured. However, no ν(CO) band could be observed near 2100 cm^{-1} in this case, in contrast to other complexes containing L1′′, L1′, and L1 ligands (see Table S1 in the Supporting Information). An additional IR spectrum was therefore measured in situ to investigate possible CO desorption under vacuum. This spectrum showed very weak ν(CO) bands at 2074 and 2100 cm^{-1} indicative of carbonyl complexes (see Figure S5 in the Supporting Information).[31] These results indicate that complex **7** is poorly reactive towards CO and that the resulting carbonyl complex cannot be isolated (Scheme 4).

Replacement of argon gas by oxygen and stirring the solution for a few hours at –78 °C produced no color change. However, the color of this solution changed gradually from colorless to deep green upon warming to room temperature. After stirring for one day, the UV/Vis and ESR spectra were measured. As shown in Figure S6 (Supporting Information), the UV/Vis spectra show a shoulder assignable to a LMCT transition from hydroxide to the copper(II) ion at 311 nm, which is a characteristic absorption band of hydroxocopper(II) complexes.[54] In addition, the d–d transition is observed at 687 nm, which is typical for five-coordinate binuclear copper(II) complexes (see Table S2 in the Supporting Information). The ESR spectra of this solution are nearly ESR-silent because of highly antiferromagnetic coupling between two copper(II) ions. On the basis of these data, it seems that a binuclear bis(μ-hydroxo)copper(II) complex is mainly produced by the reaction of complex **7** with O$_2$ (see Figure S7 in the Supporting Information). Unfortunately, no oxygenated intermediate could be isolated (Scheme 4).

In the case of L0N4, unlike L1′′, L1′, tpa, and so on, the copper(I) complex **7** hardly reacts with CO, although it reacts almost completely with PPh$_3$. This poor reactivity toward to CO also explains the fact that acetonitrile does not coordinate to the copper(I) ion in complex **7**. In addition, although complex **7** reacts with O$_2$, no stable copper–oxygen complexes are observed even at low temperature, as is also the case for L1′′. One possibility to explain this oxygen reactivity is that copper–oxygen intermediates with L0N4 are too unstable and decomposition of this species to yield copper(II) complexes is always faster than its

generation.[20] Considering these results, the related unsubstituted pyrazolyl ligand LnN4 was synthesized to increase the reactivity and investigate the reactivity of its copper(I) complex toward O_2. In fact, high reactivities of copper(I) complexes containing unsubstituted N4-type ligands (tpa etc.) with small molecules have been reported.[22,23] A dichloromethane solution containing both LnN4 and $[Cu(CH_3CN)_4](PF_6)$ was treated with O_2 at around –50 °C. Unlike the case of L0N4, the color of this solution changed immediately from colorless to deep blue, thus indicating that a copper–oxygen intermediate had formed. We are currently trying to determine the structure of this copper(II) oxygen complex.

Conclusions

Novel copper(II) and copper(I) complexes containing the neutral tripodal tetradentate nitrogen-containing ligands L0N4 and L1N4 have been systematically synthesized and characterized, and the reactivity of their copper(I) complexes investigated. The structures, properties, and reactivities observed have been compared to the corresponding complexes with the related neutral bidentate (L1′′), tridentate (L1′), and other tetradentate ligands.

As regards the structures of the synthesized copper(II) complexes, the coordination modes of the N4-type ligands in the chloro complexes **1** and **2** are different from those in complexes **3**–**6** in the sense that one pyrazolyl arm does not coordinate. A different coordination geometry due to the different methyl and isopropyl substituents of the pyrazolyl moieties is observed in the nitrato complexes **3** and **4**, whereas this is not observed in the chlorido complexes **1** and **2** or the sulfato complexes **5** and **6**. The UV/Vis and ESR spectra suggest that the structure of complex **3** is close to square pyramidal, in agreement with the other five complexes **1**, **2**, and **4**–**6** in solution. In light of this observation, and the fact that the colors of all the synthesized copper(II) complexes change upon treatment with CsI, it seems likely that the coordination abilities of L0N4 and L1N4 are somewhat lower due to the existence of tertiary amine nitrogen atoms.

As for the synthesized copper(I) complexes, the structure of the triphenylphosphane complex **8** was determined by X-ray crystallography, while that of **7** was estimated from spectroscopic and elemental analysis data, which confirm the lack of a coordinated acetonitrile in complex **7**. One pyrazolyl arm of the L0N4 ligand in complex **8** remains uncoordinated, similar to analogous complexes which have already been reported. As is the case with the N2-type complexes, the copper(I) ion lies in a trigonal plane consisting of two pyrazolyl nitrogen atoms of L0N4 and one phosphorus atom of the PPh_3 molecule. However, unlike in the N2-type complexes, an interaction between the copper(I) ion and a tertiary amine nitrogen atom of L0N4 is also observed. The ^1H and ^{31}P NMR spectra suggest that the coordination mode of complex **8** determined from the crystal structure is not maintained in solution at room temperature.

Finally, despite its bulkiness, PPh_3 reacts with complex **7** while CO hardly reacts. This instability of the copper(I) carbonyl complex containing an N4-type ligand differs from the situation found for other N2- and N3-type ligands as their carbonyl copper(I) complexes are very stable and easy to synthesize.[20,52,53,55,56] The reaction of **7** with O_2 does not produce any stable copper–oxygen complexes. The systematic results discussed above indicate a special chemistry for copper complexes of N4 ligands, therefore these findings will be applied to the search for new biologically inspired oxidation catalysts.[57]

Experimental Section

Materials: Preparation and handling of all complexes was performed under argon by employing standard Schlenk tube techniques or in a VAC inert atmosphere glovebox containing argon. Dichloromethane and acetonitrile were carefully purified by refluxing and distilling under argon over phosphorus pentoxide and over calcium hydride, respectively. Heptane was carefully purified by refluxing/distilling under argon over sodium benzophenone ketyl.[58] Methanol, ethanol, 2-propanol, acetone, chloroform, and octane were spectroscopic grade and were used after bubbling with argon. Anhydrous solvents and $[Cu(CH_3CN)_4](PF_6)$ were purchased from Aldrich Chemical Company, Inc. and stored in a glove box. Copper(I) chloride was purified according to a published method.[53] Pyrazole and 3,5-dimethylpyrazole were purchased from Aldrich Chemical Company, Inc. and Tokyo Kasei Kogyo Co., Ltd., respectively and were used without further purification. Deuterated solvents for NMR measurements were obtained from Cambridge Isotope Laboratories, Inc. Other reagents were purchased from Wako Pure Chemical Ind. Ltd. and used without further purification. $[Cu(CH_3CN)_4](ClO_4)$,[59] 3,5-diisopropylpyrazole,[53] and tris(pyrazol-1-ylmethyl)amine[39] were synthesized according to published methods. The reported copper(I) complexes $[Cu\{HC(3,5\text{-}i\mathrm{Pr}_2pz)_3\}(PPh_3)](ClO_4)$ $[\{Cu(L1')(PPh_3)\}(ClO_4)]$,[20] $[Cu\{HC(3,5\text{-}i\mathrm{Pr}_2pz)_3\}(CO)](PF_6)$ $[\{Cu(L1')(CO)\}(PF_6)]$,[12] $[Cu\{H_2C(3,5\text{-}i\mathrm{Pr}_2pz)_2\}]_2(ClO_4)_2$ $[\{Cu(L1'')\}_2(ClO_4)_2]$,[20] and $[Cu\{H_2C(3,5\text{-}i\mathrm{Pr}_2pz)_2\}(PPh_3)](ClO_4)$ $[\{Cu(L1'')(PPh_3)\}(ClO_4)]$[20] were prepared by published methods.

Caution! Perchlorate salts are potentially explosive and should be handled with care.

Measurements: IR and far-IR spectra were recorded as KBr pellets in the 4000–400 cm^{-1} region or in Nujol in the 650–150 cm^{-1} region, respectively, using a JASCO FT/IR-550 spectrophotometer. For in situ IR spectroscopy, the sample solution was stirred in a Schlenk tube, purged with carbon monoxide for a few minutes, and then stirred for one day at room temperature. This solution was then transferred to a Spectralys Specac KBr plate solution IR cell. ^1H (600 MHz), ^{13}C (150 MHz), and ^{31}P NMR (242 MHz) spectra were recorded with a Bruker AVANCE-600 NMR spectrometer at room temperature (296 K) unless stated otherwise. ^1H NMR (270 MHz) spectra were recorded with a JEOL EX-270 NMR spectrometer at room temperature (296 K) unless stated otherwise. ^1H and ^{13}C chemical shifts are reported as δ values downfield from the internal standard tetramethylsilane and the residual solvent peak. ^{31}P chemical shifts are referenced relative to an external standard of PPh_3 (δ = 0 ppm). ESR spectra were recorded with a Bruker EMXT ESR spectrometer as frozen solutions at around 123 K in quartz tubes (diameter 5 mm) using the liquid-nitrogen temperature controller BVT 3000. UV/Vis absorption spectra at room tem-

perature in the 240–1840 nm region were recorded with a JASCO V-570 spectrophotometer. Elemental analyses (C, H, N) were performed at the Department of Chemistry of the University of Tsukuba.

Ligand Preparation

Tris(3,5-dimethylpyrazol-1-ylmethyl)amine (L0N4): L0N4 and a precursor of L0N4 [1-(hydroxymethyl)-3,5-dimethyl-1-pyrazole] were prepared by a modification of the reported methods.[38,60] Thus, a 37% solution of formalin (3.0 mL, 39 mmol) in water (20 mL) was added to a solution of 3,5-dimethyl-1-pyrazole (3.27 g, 34 mmol) in 1:2 water/ethanol (30 mL). After stirring for 2 d at room temperature, the mixture was extracted with three 25-mL portions of chloroform and the organic solvent removed under reduced pressure. Crystallization from dichloromethane/toluene (1:3) yielded colorless crystals (2.71 g, 63% yield). ^{1}H NMR ($CDCl_3$, 270 MHz): δ = 2.19 (s, 3 H, CH_3), 2.34 (s, 3 H, CH_3), 5.40 (d, J = 5 Hz, 2 H, CH_2), 5.83 [s, 1 H, 4-*H*(pz)], 7.64 (br., 1 H, O*H*) ppm. FT-IR (KBr): $\tilde{\nu}$ = 3152 (s), 2118 (m), 1555 (s), 1462 (m), 1395 (m), 1308 (s), 1261 (w), 1227 (s), 1165 (m), 1068 (s), 1038 (m), 1007 (m), 985 (m), 806 (s), 759 (m), 705 (s), 634 (m), 472 (s), 448 (s), 407 (s) cm^{-1}.

1-(Hydroxymethyl)-3,5-dimethyl-1-pyrazole (1.89 g, 15 mmol) and ammonium acetate (0.39 g, 5.1 mmol) were stirred for one day at room temperature in acetonitrile (30 mL). The organic solvent was then removed under reduced pressure to give a colorless oil. Slow crystallization from methanol/water (1:1) gave colorless crystals (1.27 g, 74% yield). $C_{18}H_{27}N_7$ (341.15): calcd. C 63.32, H 7.97, N 28.71; found C 63.31, H 8.08, N 28.79. ^{1}H NMR ($CDCl_3$, 600 MHz): δ = 1.83 (s, 9 H, CH_3), 2.19 (s, 9 H, CH_3), 4.97 (s, 6 H, CH_2), 5.78 [s, 3 H, 4-*H*(pz)] ppm. ^{13}C NMR ($CDCl_3$, 150 MHz): δ = 9.8 (*C*H$_3$), 13.3 (*C*H$_3$), 62.4 (*C*H$_2$), 106.0 [4-*C*(pz)], 140.0 [3-*C*(pz)], 147.5 [5-*C*(pz)] ppm. FT-IR (KBr): $\tilde{\nu}$ = 2921 (s), 1553 (vs), 1465 (s), 1256 (s), 1199 (s), 1098 (s), 1030 (s), 974 (s), 862 (m), 787 (s), 707 (m), 628 (s), 460 (m), 430 (m), 414 (s) cm^{-1}.

Tris(3,5-diisopropylpyrazol-1-ylmethyl)amine (L1N4): L1N4 and a precursor of L1N4 [1-(hydroxymethyl)-3,5-diisopropyl-1-pyrazole] were prepared in a similar manner to L0N4 and its precursor. Thus, a 37% solution of formalin (2.0 mL, 26 mmol) in water (20 mL) was added to a solution of 3,5-diisopropyl-1-pyrazole (3.99 g, 26 mmol) in 1:3 water/ethanol (40 mL). After stirring for 3 d in a water bath at about 40 °C, the mixture was extracted with three 25-mL portions of dichloromethane and the organic solvent removed under reduced pressure. Further purification was not possible. ^{1}H NMR ($CDCl_3$, 270 MHz): δ = 1.12 [d, J = 6.9 Hz, 6 H, CH(CH_3)$_2$], 1.22 [d, J = 6.8 Hz, 6 H, CH(CH_3)$_2$], 2.82 [sept, J = 6.9 Hz, 1 H, C*H*(CH$_3$)$_2$], 3.02 [sept, J = 6.8 Hz, 1 H, C*H*(CH$_3$)$_2$], 5.40 (s, 2 H, CH_2), 5.80 [s, 1 H, 4-*H*(pz)], 7.26 (br., 1 H, O*H*) ppm. FT-IR (KBr): $\tilde{\nu}$ = 3183 (s), 2964 (s), 1545 (m), 1466 (m), 1398 (w), 1365 (w), 1289 (m), 1261 (s), 1179 (m), 1063 (s), 794 (vs), 723 (w) cm^{-1}.

Acetonitrile (40 mL) was added to a mixture of 1-(hydroxymethyl)-3,5-diisopropyl-1-pyrazole (2.73 g, 15 mmol) and ammonium acetate (0.39 g, 5.1 mmol) and the solution stirred for 2 d at about 50 °C. The solvent was then removed under reduced pressure to yield a white oil. Crystallization from a slowly cooled dichloromethane/acetonitrile (1:10) solution gave colorless crystals (2.11 g, 83% yield). $C_{30}H_{51}N_7$ (509.77): calcd. C 70.68, H 10.08, N 19.23; found C 70.56, H 10.22, N 19.15. ^{1}H NMR ($CDCl_3$, 600 MHz): δ = 0.96 [d, J = 6.8 Hz, 18 H, CH(CH_3)$_2$], 1.23 [d, J = 6.9 Hz, 18 H, CH(CH_3)$_2$], 2.22 [sept, J = 6.8 Hz, 3 H, C*H*(CH$_3$)$_2$], 2.91 [sept, J = 6.9 Hz, 3 H, C*H*(CH$_3$)$_2$], 5.03 (s, 6 H, CH_2), 5.84 [s, 3 H, 4-*H*(pz)] ppm. ^{13}C NMR ($CDCl_3$, 150 MHz): δ = 22.7 [CH(*C*H$_3$)$_2$], 22.8 [CH(*C*H$_3$)$_2$], 24.3 [*C*H(CH$_3$)$_2$], 27.8 [*C*H(CH$_3$)$_2$], 62.5 (*C*H$_2$), 99.1 [4-*C*(pz)], 150.9 [3-*C*(pz)], 158.2 [5-*C*(pz)] ppm. FT-IR (KBr): $\tilde{\nu}$ = 2963 (s), 1546 (s), 1458 (s), 1381 (s), 1297 (s), 1261 (vs), 1249 (m), 1180 (m), 1124 (s), 1063 (s), 996 (m), 963 (m), 867 (w), 835 (m), 801 (s) cm^{-1}.

Complex Preparation

[Cu^{II}(L0N4)Cl$_2$] (1): A solution of L0N4 (0.170 g, 0.498 mmol) in methanol (10 mL) was added to a solution of $CuCl_2 \cdot 2H_2O$ (0.085 g, 0.50 mmol) in the same solvent (5 mL). The color of the solution gradually turned to light green. After stirring for 1 h, the solvent was removed under reduced pressure. Crystallization from dichloromethane/octane (1:3) at –30 °C gave **1**·0.4CH_2Cl_2 as light green crystals (0.114 g, 45% yield). $C_{18.4}H_{27.8}Cl_{2.8}CuN_7$ (509.88): calcd. C 43.34, H 5.50, N 19.23; found C 43.00, H 5.82, N 19.47. FT-IR (KBr): $\tilde{\nu}$ = 2971 (w), 1629 (m), 1555 (s), 1493 (w), 1469 (m), 1421 (w), 1400 (w), 1315 (m), 1278 (m), 1055 (w), 1040 (m), 986 (s), 873 (m), 825 (w), 789 (s) cm^{-1}. Far-IR (Nujol): $\tilde{\nu}$ = 564 (w), 526 (w), 504 (w), 439 (w), 374 (m), 332 (m), 351 (w), 310 (m), 295 (s), 288 (s), 278 (m), 245 (m), 176 (w) cm^{-1}. UV/Vis (dichloromethane): λ (ε) = 858 nm (270 M^{-1} cm^{-1}), 356 (1510), 279 (4290). ESR (methanol/ethanol = 9:1, 123 K): $g_{\|}$ = 2.30 ($A_{\|}$ = 136 G); $g_{\perp}$ = 2.07.

[Cu^{II}(L1N4)Cl$_2$] (2): This complex was synthesized in the same manner as **2** using $CuCl_2 \cdot 2H_2O$ (0.068 g, 0.40 mmol) in methanol (5 mL) and L1N4 (0.201 g, 0.394 mmol) in methanol (10 mL). Crystallization from chloroform/heptane (1:4) at –50 °C gave light green crystals (0.071 g, 28% yield). $C_{30}H_{51}Cl_2CuN_7$ (644.22): calcd. C 55.93, H 7.98, N 15.22; found C 55.73, H 7.99, N 15.14. FT-IR (KBr): $\tilde{\nu}$ = 2966 (s), 2930 (w), 2871 (w), 1633 (w), 1547 (s), 1469 (m), 1410 (m), 1384 (m), 1367 (w), 1317 (w), 1273 (m), 1261 (m), 1183 (m), 1086 (m), 1062 (s), 1023 (m), 800 (vs) cm^{-1}. Far-IR (Nujol): $\tilde{\nu}$ = 577 (w), 547 (w), 513 (w), 472 (w), 456 (w), 396 (w), 309 (s), 246 (m), 227 (w) cm^{-1}. UV/Vis (dichloromethane): λ (ε) = 847 nm (270 M^{-1} cm^{-1}), 354 (1840), 280 (5120). ESR (methanol/ethanol = 9:1, 123 K): $g_{\|}$ = 2.29 ($A_{\|}$ = 141 G); $g_{\perp}$ = 2.07.

[Cu^{II}(L0N4)(NO$_3$)](NO$_3$) (3): A solution of L0N4 (0.171 g, 0.500 mmol) in methanol (10 mL) was added to a solution of $Cu(NO_3)_2 \cdot 3H_2O$ (0.121 g, 0.501 mmol) in methanol (7 mL). The color of the solution gradually turned to bluish green. After stirring for 1 h, the solution was concentrated under reduced pressure. Crystallization from methanol at –30 °C gave green crystals (0.190 g, 72% yield). $C_{18}H_{27}CuN_9O_6$ (529.01): calcd. C 40.87, H 5.14, N 23.8; found C 40.76, H 5.00, N 23.67. FT-IR (KBr): $\tilde{\nu}$ = 3437 (m), 3131 (w), 2991 (w), 1557 (s), 1495 (s), 1469 (s), 1385 (vs), 1359 (s), 1332 (m), 1290 (s), 1119 (w), 1058 (m), 1004 (m), 797 (w) cm^{-1}. Far-IR (Nujol): $\tilde{\nu}$ = 625 (w), 594 (w), 558 (w), 541 (w), 500 (w), 438 (m), 356 (w), 324 (m), 301 (w), 245 (w) cm^{-1}. UV/Vis (dichloromethane): λ (ε) = 312 nm (1530 M^{-1} cm^{-1}), 756 (100). ESR (methanol/ethanol = 9:1, 123 K): $g_{\|}$ = 2.30 ($A_{\|}$ = 140 G); $g_{\perp}$ = 2.08.

[Cu^{II}(L1N4)(NO$_3$)](NO$_3$) (4): This complex was synthesized in the same manner as **3** using $Cu(NO_3)_2 \cdot 3H_2O$ (0.123 g, 0.509 mmol) in methanol (5 mL) and L1N4 (0.255 g, 0.500 mmol) in methanol (15 mL). Crystallization from methanol/2-propanol (1:3) at –30 °C gave bluish green crystals (0.125 g, 36% yield). $C_{30}H_{51}CuN_9O_6$ (697.33): calcd. C 51.67, H 7.37, N 18.08; found C 51.56, H 7.27, N 17.78. FT-IR (KBr): $\tilde{\nu}$ = 3443 (m), 2967 (s), 2933 (w), 2871 (w), 1548 (m), 1498 (m), 1473 (m), 1384 (vs), 1276 (m), 1188 (w), 1061 (w), 1000 (w), 800 (w) cm^{-1}. Far-IR (Nujol): $\tilde{\nu}$ = 612 (s), 578 (w), 522 (w), 493 (w), 472 (w), 432 (w), 395 (w), 333 (m), 306 (w), 257 (m) cm^{-1}. UV/Vis (dichloromethane): λ (ε) = 302 nm (1580 M^{-1} cm^{-1}), 748 (130). ESR (methanol/ethanol = 9:1, 123 K): $g_{\|}$ = 2.29 ($A_{\|}$ = 132 G); $g_{\perp}$ = 2.08.

[Cu^{II}(L0N4)(SO_4)] (5): A solution of L0N4 (0.171 g, 0.501 mmol) in methanol (10 mL) was added to a solution of $CuSO_4 \cdot 5H_2O$ (0.124 g, 0.497 mmol) in methanol (5 mL). The color of the solution gradually turned to deep blue. After stirring for 1 h, the solution was concentrated under reduced pressure. Crystallization from methanol/ethanol (1:3) at –30 °C gave **5**·H_2O as blue crystals (0.104 g, 40% yield). $C_{18}H_{29}CuN_7O_5S$ (519.08): calcd. C 41.65, H 5.63, N 18.89; found C 41.84, H 5.59, N 19.13. FT-IR (KBr): $\tilde{\nu}$ = 3434 (s), 3127 (w), 2922 (m), 1556 (s), 1468 (m), 1422 (m), 1397 (m), 1314 (w), 1280 (m), 1209 (s), 1141 (vs), 1039 (s), 957 (s), 930 (m), 884 (w), 785 (w), 651 (m) cm^{-1}. Far-IR (Nujol): $\tilde{\nu}$ = 600 (w), 507 (m), 471 (w), 449 (m), 364 (w), 333 (m), 299 (s), 253 (w), 245 (w), 206 (w) cm^{-1}. UV/Vis (dichloromethane): λ (ε) = 286 nm (4650 $M^{-1}cm^{-1}$), 699 (90). ESR (methanol/ethanol = 9:1, 123 K): $g_{\parallel}$ = 2.30 ($A_{\parallel}$ = 141 G); $g_{\perp}$ = 2.08.

[Cu^{II}(L1N4)(SO_4)] (6): This complex was synthesized in the same manner as **5** using $CuSO_4 \cdot 5H_2O$ (0.125 g, 0.501 mmol) in methanol (5 mL) and L1N4 (0.255 g, 0.500 mmol) in methanol (10 mL). Crystallization from methanol at –50 °C gave **6**·0.75H_2O as blue crystals (0.134 g, 39% yield). $C_{30}H_{52.5}CuN_7O_{4.75}S$ (682.89): calcd. C 52.76, H 7.75, N 14.36; found C 52.62, H 7.47, N 14.34. FT-IR (KBr): $\tilde{\nu}$ = 3433 (m), 3192 (w), 2966 (s), 2871 (w), 1547 (m), 1472 (m), 1384 (w), 1368 (w), 1263 (m), 1183 (m), 1117 (vs), 1029 (s), 970 (w), 798 (s), 661 (m), 620 (m) cm^{-1}. Far-IR (Nujol): $\tilde{\nu}$ = 583 (m), 522 (w), 495 (m), 480.2 (m), 433 (w), 393 (w), 311 (s), 278 (m), 253 (m), 196 (w) cm^{-1}. UV/Vis (dichloromethane): λ (ε) = 703 nm (140 $M^{-1}cm^{-1}$), 275 (4260). ESR (methanol/ethanol = 9:1, 123 K): $g_{\parallel}$ = 2.33 ($A_{\parallel}$ = 126 G); $g_{\perp}$ = 2.07.

[Cu^{I}(L0N4)](PF_6) (7): A solution of L0N4 (0.153 g, 0.448 mmol) in methanol (10 mL) was added to a solution of [$Cu(CH_3CN)_4$](PF_6) (0.168 g, 0.451 mmol) in methanol (20 mL). After stirring for 2 h, the suspension was filtered and the resulting white solid washed with methanol (20 mL) and dichloromethane (20 mL). After drying under reduced pressure, **7**·0.2CH_2Cl_2 was obtained as a white powder (0.208 g, 82% yield). $C_{18.2}H_{27.4}Cl_{0.4}CuF_6N_7P$ (566.95): calcd. C 38.56, H 4.87, N 17.29; found C 38.55, H 4.88, N 17.33. FT-IR (KBr): $\tilde{\nu}$ = 3430 (w), 2981 (w), 2927 (w), 1635 (w), 1557 (s), 1465 (m), 1428 (m), 1389 (m), 1308 (m), 1247 (m), 1196 (w), 1108 (m), 1094 (m), 1045 (m), 842 (vs), 713 (m), 557 (s) cm^{-1}. Far-IR (CsI): $\tilde{\nu}$ = 558 (s), 535 (m), 504 (m), 494 (w), 472 (m), 415 (w), 374 (w), 340 (w), 292 (m), 212 (m) cm^{-1}. ^{1}H NMR (CD_3CN, 600 MHz): δ = 2.09 (s, 9 H, CH_3), 2.24 (s, 9 H, CH_3), 4.95 [s, 3 H, 4-*H*(pz)], 5.99 (s, 6 H, H_2C) ppm. ^{13}C NMR (CD_3CN, 150 MHz): δ = 10.5 (*C*H_3), 13.3 (*C*H_3), 61.6 (*C*H_2), 107.0 [4-*C*(pz)], 141.6 [3-*C*(pz)], 149.3 [5-*C*(pz)] ppm.

[Cu^{I}(L0N4)(PPh_3)](ClO_4) (8): A solution of PPh_3 (0.057 g, 0.217 mmol) in dichloromethane (15 mL) was added to solid **7** (0.120 g, 0.218 mmol). After stirring for 3 h, $NaClO_4 \cdot H_2O$ (0.027 g, 0.192 mmol) dissolved in acetone (5 mL) was added to the solution. After stirring for 3 h, the solution was dried under reduced pressure and the complex extracted with dichloromethane (20 mL). The solution was filtered and the filtrate concentrated under reduced pressure. Crystallization from dichloromethane/hexane (1:3) at –50 °C gave **8**·0.3CH_2Cl_2 as colorless crystals (0.074 g, 43% yield). $C_{36.3}H_{42.6}Cl_{1.6}CuN_7O_4P$ (792.22): calcd. C 55.03, H 5.42, N 12.38; found C 55.12, H 5.66, N 12.15. FT-IR (KBr): $\tilde{\nu}$ = 3458 (m), 2954 (w), 2919 (w), 1558 (m), 1464 (w), 1435 (m), 1393 (w), 1331 (m), 1259 (w), 1237 (w), 1095 (vs), 747 (s), 696 (s), 622 (m), 530 (m) cm^{-1}. Far-IR (CsI): $\tilde{\nu}$ = 623 (s), 531 (s), 499 (s), 472 (w), 445 (m), 395 (w), 378 (m), 344 (w), 332 (w), 318 (w), 276 (m), 203 (m), 194 (m) cm^{-1}. ^{1}H NMR (CD_3CN, 600 MHz): δ = 2.14 (s, 9 H, CH_3), 2.19 (s, 9 H, CH_3), 4.82 [s, 3 H, 4-*H*(pz)], 6.01 (s, 6 H, H_2C), 7.34–7.63 (m, 15 H, P*Ph*$_3$) ppm. ^{13}C NMR (CD_3CN, 150 MHz): δ = 10.9 (*C*H_3), 13.9 (*C*H_3), 62.0 (*C*H_2), 107.0 [4-*C*(pz)], 129.8 (P*Ph*$_3$), 131.1 (P*Ph*$_3$), 132.6 (P*Ph*$_3$), 132.8 (P*Ph*$_3$), 133.6 (P*Ph*$_3$), 133.7 (P*Ph*$_3$), 142.3 [3-*C*(pz)], 149.7 [5-*C*(pz)] ppm. ^{31}P NMR ($CDCl_3$, 242 MHz): δ = 2.75 (br. s, *P*Ph_3) ppm.

Reaction of 7 with CO: Complex **7** was dissolved in dichloromethane in a Schlenk tube and cooled to –78 °C under argon. The argon was then replaced with carbon monoxide and the solution warmed

Table 7. Crystallographic data for L0N4, L1N4, and complexes **1** and **2**.

Compound	L0N4·7H_2O	L1N4	**1**·2CH_2Cl_2	**2**·$CHCl_3$
Formula	$C_{18}H_{35}N_7O_7$	$C_{30}H_{51}N_7$	$C_{20}H_{31}Cl_6CuN_7$	$C_{33}H_{54}Cl_{11}CuN_7$
F.W.	461.52	509.78	645.78	1002.37
Crystal system	triclinic	triclinic	triclinic	monoclinic
Space group	$P\bar{1}$ (No. 2)	$P\bar{1}$ (No. 2)	$P\bar{1}$ (No. 2)	$P2_1/n$ (No. 14)
a [Å]	10.9826(4)	9.6471(2)	8.5775(2)	15.4577(5)
b [Å]	10.9868(2)	9.8740(4)	13.2652(2)	22.3605(5)
c [Å]	11.0067(2)	16.4202(5)	13.2749(4)	15.5845(5)
α [°]	79.610(8)	83.100(4)	85.477(5)	90
β [°]	79.621(8)	79.058(4)	82.995(4)	113.9590(4)
γ [°]	79.782(8)	86.874(5)	76.929(4)	90
V [Å^3]	1270.46(6)	1523.75(8)	1458.28(6)	4922.5(2)
Z	2	2	2	4
D_{calc} [g cm^{-3}]	1.206	1.111	1.471	1.352
μ(Mo-K_α) [cm^{-1}]	0.934	0.675	13.206	10.708
Temp. [°C]	–80	–80	–90	–90
Reflections collected	10316	12258	11926	38486
R_{int}	0.020	0.022	0.018	0.034
Unique reflections	5652	6746	6602	11167
Number of observations [$I > 3.0\sigma(I)$]	4188	4350	5755	6772
Number of variables	324	385	338	523
Final *R* (*R*w)[a]	0.0736 (0.1068)	0.0760 (0.1065)	0.0452 (0.0688)	0.0590 (0.0766)
GOF	1.707	1.613	1.250	1.149
Max./min. peak [e/Å^3]	0.80/–0.39	0.36/–0.35	1.40/–1.09	0.92/–0.65

[a] $R = \sum||F_o| - |F_c||/\sum|F_o|$; $Rw = [(|F_o| - |F_c|)^2/\sum wF_o^2]^{1/2}$, $w = 1/\sigma^2(|F_o|)$.

Table 8. Crystallographic data for complexes **3**–**6** and **8**.

Compound	**3**	**4**·EtOH	**5**·2EtOH·0.5MeOH	**6**·7MeOH	**8**·CH_2Cl_2·MeOH
Formula	$C_{18}H_{27}CuN_9O_6$	$C_{32}H_{57}CuN_9O_7$	$C_{22.5}H_{41}CuN_7O_{6.5}S$	$C_{37}H_{79}CuN_7O_{11}S$	$C_{38}H_{48}Cl_3CuN_7O_5P$
F.W.	529.01	743.40	609.22	893.68	883.72
Crystal system	monoclinic	triclinic	monoclinic	monoclinic	triclinic
Space group	*C*2/*c* (No. 15)	$P\bar{1}$ (No. 2)	$P2_1/n$ (No. 14)	$P2_1/c$ (No. 14)	$P\bar{1}$ (No. 2)
a [Å]	25.5478(17)	10.3651(4)	8.9916(11)	12.6999(11)	13.7987(4)
b [Å]	10.3909(4)	12.5039(5)	15.8436(15)	23.3385(11)	13.9118(4)
c [Å]	20.6190(13)	14.6314(5)	19.480(3)	17.1747(15)	22.5459(5)
α [°]	90	96.036(2)	90	90	96.4240(13)
β [°]	119.9450(5)	94.195(2)	94.820(2)	106.9800(11)	94.9740(13)
γ [°]	90	97.986(2)	90	90	96.3080(13)
V [Å^3]	4742.9(5)	1860.06(12)	2765.3(6)	4868.6(6)	4253.28(20)
Z	8	2	4	4	4
D_{calc} [g cm^{-3}]	1.482	1.327	1.463	1.219	1.380
μ(Mo-K_α) [cm^{-1}]	9.742	6.438	9.178	5.489	7.888
Temp. [°C]	–90	–90	–90	–90	–89
Reflections collected	17733	15210	19861	32634	23580
R_{int}	0.029	0.017	0.054	0.041	0.067
Unique reflections	5337	8396	6137	10450	17807
Number of observations [$I > 3.0\sigma(I)$]	4347	7532	5710	8166	10148
Number of variables	334	517	395	593	1067
Final *R* (*R*w)[a]	0.0486 (0.0740)	0.0554 (0.0854)	0.0749 (0.0936)	0.0954 (0.1300)	0.0913 (0.1238)
GOF	1.357	1.599	6.785	1.980	1.582
Max./min. peak [e/Å^3]	0.61/–0.46	0.85/–0.77	0.97/–1.09	1.19/–0.94	1.79/–0.78

[a] $R = \Sigma||F_o| - |F_c||/\Sigma|F_o|$; $Rw = [(|F_o| - |F_c|)^2/\Sigma wF_o^2]^{1/2}$, $w = 1/\sigma^2(|F_o|)$.

to room temperature. After stirring for 24 h, an in situ IR spectrum of this solution was recorded.

Complex **7** was dissolved in [D_3]acetonitrile in a Schlenk tube and cooled to –78 °C under argon. The argon was then replaced with carbon monoxide and the solution warmed to room temperature. After stirring for 24 h, the ^{1}H NMR spectrum of this solution was recorded.

Reaction of 7 with O_2: Complex **7** was dissolved in dichloromethane in a Schlenk tube and cooled to –78 °C under argon. The argon was then replaced by dioxygen gas and stirred for a few hours. This solution was warmed to room temperature. After stirring for a day, the UV/Vis and ESR spectra of this solution were recorded.

X-ray Data Collection and Structural Determination: The diffraction data for ligands L0N4 and L1N4 and complexes **1**–**6** and **8** were collected on a Rigaku/MSC Mercury CCD system with graphite-monochromated Mo-K_α (λ = 0.71069 Å) radiation at low temperature (Tables 7 and 8). Each crystal was mounted on the tip of a glass fiber in heavy viscous oil. The unit cell parameters of each crystal were determined from six images using Rigaku Daemon software and refined using CrystalClear.[61] Data were collected using 0.5° intervals for 30 s/frame (L0N4, **1**, **3**, **4**, **5**), 40 s/frame (L1N4, **2**), 15 s/frame (**6**), or 64 s/frame (**8**) in ϕ and ω to a maximum 2θ value of 55°. A total of 744 oscillation images were collected. The highly redundant data sets were reduced using CrystalClear and corrected for Lorentz and polarization effects. An empirical absorption correction was applied for each complex.[61–63] The structures were solved by direct methods using the programs SIR 92[64] and SIR 97.[65] The positions of the metal atoms and their first coordination sphere were located from the *E*-map; other non-hydrogen atoms were found in alternating difference Fourier syntheses.[66] Least-squares refinement cycles on *F* were conducted using CrystalStructure with anisotropic displacement parameters for non-hydrogen atoms; hydrogen atoms were placed in calculated positions.[62,63] Strong remaining peaks in complexes **1**, **2**, **5**, **6**, and **8** are due to the disordered solvents, whereas the peaks in **4** are due to the disordered nitrate ion. Two disordered MeOH molecules in **8** were refined isotropically. The high GOF value of **5** is also due to the disordered solvents. A weighting scheme (according to Sheldrick) was performed for all complexes except **5**.

CCDC-620398 (for L1N4), 620399 (for L0N4), 699107 (for **1**), 699108 (for **2**), 620400 (for **4**), 620401 (for **3**), 620402 (for **6**), 620403 (for **5**), and 699106 (for **8**) contain the crystallographic data for this paper. These data can be obtained free of charge from The Cambridge Crystallographic Data Centre via www.ccdc.cam.ac.uk/data_request/cif.

Supporting Information (see also the footnote on the first page of this article): Figures S1–S7: ORTEP drawings of L1N4, **2**, **4**, and **6**, IR and UV/Vis spectra, and proposed structure of oxygenated complex. Tables S1 and S2: IR and UV/Vis data.

Acknowledgments

This research was supported by the Japan Society for the Promotion of Science (JSPS) (Grant-in-Aid for Scientific Research (B), grant number 17350043) and from the Ministry of Education, Culture, Sports, Science and Technology (MEXT) for Scientific Research on Priority Areas "Advanced Molecular Transformations of Carbon Resources" (19020011).

[1] R. H. Holm, P. Kennepohl, E. I. Solomon, *Chem. Rev.* **1996**, *96*, 2239–2314.
[2] W. Kaim, J. Rall, *Angew. Chem. Int. Ed. Engl.* **1996**, *35*, 43–60.
[3] E. I. Solomon, P. Chen, M. Metz, S.-K. Lee, A. E. Palmer, *Angew. Chem. Int. Ed.* **2001**, *40*, 4570–4590.
[4] *Handbook of Metalloproteins* (Eds.: A. Messerschmidt, R. Huber, T. Poulos, K. Wieghardt), John Wiley & Sons, Inc., Chichester, UK, **2001**.
[5] *Handbook on Metalloproteins* (Eds.: I. Bertini, A. Sigel, H. Sigel), Marcel Dekker, Inc., New York, USA, **2001**.
[6] S. Trofimenko, *Chem. Rev.* **1993**, *93*, 943–980.

[7] N. Kitajima, W. B. Tolman, *Prog. Inorg. Chem.* **1995**, *43*, 419–531.
[8] G. Parkin, *Adv. Inorg. Chem.* **1995**, *42*, 291–393.
[9] S. Trofimenko, *Scorpionates: The Coordination Chemistry of Polypyrazolylborate Ligands*, Imperial College Press, London, UK, **1999**.
[10] G. Parkin, *Chem. Commun.* **2000**, 1971–1985.
[11] C. Pettinari, *Scorpionates II*, Imperial College Press, London, UK, **2008**.
[12] K. Fujisawa, T. Ono, Y. Ishikawa, N. Amir, Y. Miyashita, K. Okamoto, N. Lehnert, *Inorg. Chem.* **2006**, *45*, 1698–1713.
[13] S. Trofimenko, *J. Am. Chem. Soc.* **1970**, *92*, 5118–5126.
[14] K.-B. Shiu, L.-Y. Yeh, S.-M. Peng, M.-C. Cheng, *J. Organomet. Chem.* **1993**, *460*, 203–211.
[15] C.-C. Chou, C.-C. Su, H.-L. Tsai, K.-H. Lii, *Inorg. Chem.* **2005**, *44*, 628–632.
[16] C.-C. Chou, C.-C. Su, A. Yeh, *Inorg. Chem.* **2005**, *44*, 6122–6128.
[17] G. Pampaloni, R. Peloso, C. Graiff, A. Tiripicchio, *Dalton Trans.* **2006**, 3576–3583.
[18] M. J. Calhorda, P. J. Costa, O. Crespo, M. C. Gimeno, P. G. Jones, A. Laguna, M. Naranjo, S. Quintal, Y.-J. Shi, M. D. Villacampa, *Dalton Trans.* **2006**, 4104–4113.
[19] A. Boni, G. Pampaloni, R. Peloso, D. Belletti, C. Graiff, A. Tiripicchio, *J. Organomet. Chem.* **2006**, *691*, 5602–5609.
[20] K. Fujisawa, Y. Noguchi, Y. Miyashita, K. Okamoto, N. Lehnert, *Inorg. Chem.* **2007**, *46*, 10607–10623.
[21] G. Pampaloni, R. Peloso, D. Belletti, C. Graiff, A. Tiripicchio, *Organometallics* **2007**, *26*, 4278–4286.
[22] R. R. Jacobson, Z. Tyeklár, A. Farooq, K. D. Karlin, S. Liu, J. Zubieta, *J. Am. Chem. Soc.* **1988**, *110*, 3690–3692.
[23] Z. Tyeklár, R. R. Jacobson, N. Wei, N. N. Murthy, J. Zubieta, K. D. Karlin, *J. Am. Chem. Soc.* **1993**, *115*, 2677–2689.
[24] H. Hayashi, S. Fujinami, S. Nagatomo, S. Ogo, M. Suzuki, A. Uehara, Y. Watanabe, T. Kitagawa, *J. Am. Chem. Soc.* **2000**, *122*, 2124–2125.
[25] M. Mizuno, H. Hayashi, S. Fujinami, H. Furutachi, S. Nagatomo, S. Otake, K. Uozumi, M. Suzuki, T. Kitagawa, *Inorg. Chem.* **2003**, *42*, 8534–8544.
[26] K. Komiyama, H. Furutachi, S. Nagatomo, A. Hashimoto, H. Hayashi, S. Fujinami, M. Suzuki, T. Kitagawa, *Bull. Chem. Soc. Jpn.* **2004**, *77*, 59–72.
[27] C. Würtele, E. Gaoutchenova, K. Harms, M. C. Holthausen, J. Sundermeyer, S. Schindler, *Angew. Chem. Int. Ed.* **2006**, *45*, 3867–3869.
[28] N. Wei, N. N. Murthy, Q. Chen, J. Zubieta, K. D. Karlin, *Inorg. Chem.* **1994**, *33*, 1953–1965.
[29] M. Schatz, M. Becker, F. Thaler, F. Hampel, S. Schindler, R. R. Jacobson, Z. Tyeklár, N. N. Murthy, P. Ghosh, Q. Chen, J. Zubieta, K. D. Karlin, *Inorg. Chem.* **2001**, *40*, 2312–2322.
[30] C. X. Zhang, S. Kaderli, M. Costas, E.-L. Kim, Y.-M. Neuhold, K. D. Karlin, A. D. Zuberbühler, *Inorg. Chem.* **2003**, *42*, 1807–1824.
[31] H. C. Fry, H. R. Lucas, A. A. N. Sarjeant, K. D. Karlin, G. J. Meyer, *Inorg. Chem.* **2008**, *47*, 241–256.
[32] K. D. Karlin, J. C. Hayes, S. Juen, J. P. Hutchinson, J. Zubieta, *Inorg. Chem.* **1982**, *21*, 4106–4108.
[33] N. Wei, N. N. Murthy, K. D. Karlin, *Inorg. Chem.* **1994**, *33*, 6093–6100.
[34] H. Nagao, N. Komeda, M. Mukaida, M. Suzuki, K. Tanaka, *Inorg. Chem.* **1996**, *35*, 6809–6815.
[35] Z.-H. Zhang, Z.-H. Ma, Y. Tang, W.-J. Ruan, *J. Chem. Crystallogr.* **2004**, *34*, 119–125.
[36] B. Lucchese, K. J. Humphreys, D.-H. Lee, C. D. Incarvito, R. D. Sommer, A. L. Rheingold, K. D. Karlin, *Inorg. Chem.* **2004**, *43*, 5987–5998.
[37] A. Wada, Y. Honda, S. Yamaguchi, S. Nagatomo, T. Kitagawa, K. Jitsukawa, H. Masuda, *Inorg. Chem.* **2004**, *43*, 5725–5735.
[38] W. L. Driessen, *Recl. Trav. Chim. Pays-Bas* **1982**, *101*, 441–443.
[39] W. L. Driessen, W. G. R. Wiesmeijer, M. Schipper-Zablotskaja, R. A. G. de Graaff, J. Reedijk, *Inorg. Chim. Acta* **1989**, *162*, 233–238.
[40] A. W. Addison, T. N. Rao, J. Reedijk, J. van Rijn, G. C. Verschoor, *J. Chem. Soc., Dalton Trans.* **1984**, 1349–1356.
[41] N. Lehnert, U. Cornelissen, F. Neese, T. Ono, Y. Noguchi, K. Okamoto, K. Fujisawa, *Inorg. Chem.* **2007**, *46*, 3916–3933.
[42] K. Fujisawa, T. Ono, H. Aoki, Y. Ishikawa, Y. Miyashita, K. Okamoto, H. Nakazawa, H. Higashimura, *Inorg. Chem. Commun.* **2004**, *7*, 330–332.
[43] K. Fujisawa, R. Kanda, Y. Miyashita, K. Okamoto, *Polyhedron* **2008**, *27*, 1432–1446.
[44] K. Fujisawa, H. Iwamoto, K. Tobita, Y. Miyashita, K. Okamoto, *Inorg. Chim. Acta* in press.
[45] K. Fujisawa, H. Aoki, Y. Miyashita, K. Okamoto, manuscript in preparation.
[46] K. Nakamoto, *Infrared and Raman Spectra of Inorganic and Coordination Compounds*, 5th ed., John Wiley & Sons, Inc., New York, USA, **1997**.
[47] A. B. P. Lever, *Inorganic Electronic Spectroscopy*, 2nd ed., Elsevier, Amsterdam, the Netherlands, **1984**.
[48] B. J. Hathaway, *Struct. Bonding (Berlin)* **1984**, *57*, 55–118.
[49] K. Shobatake, C. Postmus, J. R. Ferraro, K. Nakamoto, *Appl. Spectrosc.* **1969**, *23*, 12–16.
[50] C. Pettinari, F. Marchetti, R. Polimante, A. Cingolani, G. Portalone, M. Colapietro, *Inorg. Chim. Acta* **1996**, *249*, 215–229.
[51] K. Uozumi, Y. Hayashi, M. Suzuki, A. Uehara, *Chem. Lett.* **1993**, *22*, 963–966.
[52] K. Fujisawa, M. Yoshida, Y. Miyashita, K. Okamoto, *Polyhedron* **2009**, *28*, 1447–1454.
[53] N. Kitajima, K. Fujisawa, C. Fujimoto, Y. Moro-oka, S. Hashimoto, T. Kitagawa, K. Toriumi, K. Tatsumi, A. Nakamura, *J. Am. Chem. Soc.* **1992**, *114*, 1277–1291.
[54] K. Fujisawa, T. Kobayashi, K. Fujita, N. Kitajima, Y. Moro-oka, Y. Miyashita, Y. Yamada, K. Okamoto, *Bull. Chem. Soc. Jpn.* **2000**, *73*, 1797–1804.
[55] S. Imai, K. Fujisawa, T. Kobayashi, N. Shirasawa, H. Fujii, T. Yoshimura, N. Kitajima, Y. Moro-oka, *Inorg. Chem.* **1998**, *37*, 3066–3070.
[56] H. V. R. Dias, C. J. Lovely, *Chem. Rev.* **2008**, *108*, 3223–3238.
[57] L. Que Jr., W. B. Tolman, *Nature* **2008**, *455*, 333–340.
[58] W. L. F. Armarego, D. D. Perrin, *Purification of Laboratory Chemicals*, 4th ed., Butterworth-Heinemann, Oxford, UK, **1997**.
[59] H.-C. Liang, K. D. Karlin, R. Dyson, S. Kaderli, B. Jung, A. D. Zuberbühler, *Inorg. Chem.* **2000**, *39*, 5884–5894.
[60] I. Dvoretzky, G. H. Richter, *J. Org. Chem.* **1950**, *15*, 1285–1288.
[61] *CrystalClear Ver. 1.3.*, J. W. Pflugrath, *Acta Crystallogr., Sect. D* **1999**, *55*, 1718–1725.
[62] *CrystalStructure 3.8*, Crystal Structure Analysis Package, Rigaku and Rigaku/MSC, **2007**.
[63] *Crystal Issue 11*: J. R. Carruthers, J. S. Rollett, P. W. Betteridge, D. Kinna, L. Pearce, A. Larsen, E. Gabe, Chemical Crystallography Laboratory, Oxford, UK, **1996**.
[64] *SIR 92*: A. Altomare, G. Cascarano, C. Giacovazzo, A. Guagliardi, *J. Appl. Crystallogr.* **1993**, *26*, 343–350.
[65] *SIR 97*: A. Altomare, M. C. Burla, M. Camalli, G. L. Cascarano, C. Giacovazzo, A. Guagliardi, A. G. G. Moliterni, G. Polidori, R. Spagna, *J. Appl. Crystallogr.* **1999**, *32*, 115–119.
[66] *DIRDIF-99*: P. T. Beurskens, G. Admiraal, G. Beurskens, W. P. Bosman, R. de Gelder, R. Israel, J. M. M. Smits, Technical Report of the Crystallography Laboratory, University of Nijmegen, The Netherlands, **1999**.

Received: May 1, 2009
Published Online: July 29, 2009

